

AD-767 258

THE EFFECT OF WRAP-AROUND FINS ON
AERODYNAMIC STABILITY AND ROLLING
MOMENT VARIATIONS

C. W. Dahlke, et al

Army Missile Command
Redstone Arsenal, Alabama

20 July 1973

DISTRIBUTED BY:

NTIS

National Technical Information Service
U. S. DEPARTMENT OF COMMERCE
5285 Port Royal Road, Springfield Va. 22151

AD 767258

AD

TECHNICAL REPORT

RD-73-17

THE EFFECT OF WAP-AROUND FINS ON AERODYNAMIC
STABILITY AND ROLLING MOMENT VARIATIONS

by

C. W. Dahlke

J. C. Craft

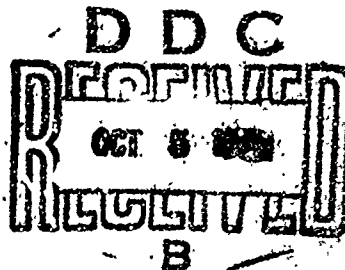
JULY 1973

Approved for public release; distribution unlimited.



U.S. ARMY MISSILE COMMAND

Redstone Arsenal, Alabama



Reproduced by
NATIONAL TECHNICAL
INFORMATION SERVICE

U S Department of Commerce
Springfield VA 22151

DISPOSITION INSTRUCTIONS

DESTROY THIS REPORT WHEN IT IS NO LONGER NEEDED. DO NOT
RETURN IT TO THE ORIGINATOR.

DISCLAIMER

THE FINDINGS IN THIS REPORT ARE NOT TO BE CONSTRUED AS AN
OFFICIAL DEPARTMENT OF THE ARMY POSITION UNLESS SO DESIGNATED
BY OTHER AUTHORIZED DOCUMENTS.

TRADE NAMES

USE OF TRADE NAMES OR MANUFACTURERS IN THIS REPORT DOES
NOT CONSTITUTE AN OFFICIAL INDORSEMENT OR APPROVAL OF
THE USE OF SUCH COMMERCIAL HARDWARE OR SOFTWARE.

ACCESSION FOR	
NTIS	Write Section <input checked="" type="checkbox"/>
DIC	Ref. Section <input type="checkbox"/>
DMC	<input type="checkbox"/>
Jou. In. Section	
BY	
DISTRIBUTION/AVAILABILITY CODES	
Dist.	AVAIL. 224/27 SPECIAL
A	

UNCLASSIFIED

Security Classification

DOCUMENT CONTROL DATA - R & D

(Security classification of title, body of abstract and indexing annotation must be entered when the overall report is classified)

1. ORIGINATING ACTIVITY (Corporate author) US Army Missile Research, Development and Engineering Laboratory US Army Missile Command Redstone Arsenal, Alabama 35809		2a. REPORT SECURITY CLASSIFICATION Unclassified	
		2b. GROUP NA	
3. REPORT TITLE THE EFFECT OF WRAP-AROUND FINS ON AERODYNAMIC STABILITY AND ROLLING MOMENT VARIATIONS			
4. DESCRIPTIVE NOTES (Type of report and inclusive dates) Technical Report			
5. AUTHOR(S) (First name, middle initial, last name) C. W. Dahlke and J. C. Craft			
6. REPORT DATE 20 July 1973		7a. TOTAL NO. OF PAGES 53	7b. NO. OF REFS 7
8a. CONTRACT OR GRANT NO.		9a. ORIGINATOR'S REPORT NUMBER(S) RD-73-17	
b. PROJECT NO. (DA) 1M262303A214			
c. AMC Management Structure Code No. 632303.11.21405		9b. OTHER REPORT NO(S) (Any other numbers that may be assigned this report) AD _____	
d.			
10. DISTRIBUTION STATEMENT Approved for public release; distribution unlimited.			
11. SUPPLEMENTARY NOTES None		12. SPONSORING MILITARY ACTIVITY Same as No. 1	
13. ABSTRACT This report presents the results of an investigation of the effect of wrap-around fins on missile rolling moment coefficient. This investigation was conducted for four fin configurations at free stream Mach numbers ranging from 0.3 to 2.86. The wrap-around fin was found to have a self induced roll moment at zero angle of attack that varies with Mach number. This effect was studied for several fin geometric configurations for the static moment case. Comparisons between the moments caused by the fin cant and wrap-around fins are shown for the rolling case.			

DD FORM 1473
1 NOV 65REPLACES DD FORM 1473, 1 JAN 64, WHICH IS
OBSOLETE FOR ARMY USE.

UNCLASSIFIED

Security Classification

UNCLASSIFIED

Security Classification

14. KEY WORDS	LINK A		LINK B		LINK C	
	ROLE	WT	ROLE	WT	ROLE	WT
Wrap-around fins Missile rolling moment coefficient Free stream Mach numbers						

UNCLASSIFIED

Security Classification

CONTENTS

	Page
1. Introduction	2
2. Discussion of Test Conducted and Model	2
3. Comparison of WAF to Flat Fin Stability and Drag	3
4. Rolling Moment Coefficient	4
5. Accuracy of Rolling Moment Coefficient Data	6
6. Side Forces and Moments	8
7. Typical Missile Roll Rate with WAF	8
8. Conclusions	9
References	51

1. Introduction

The military services have been interested for some time in missile designs that have tube-launched applications. Wrap-around fins (WAF) have always been a promising means of stabilizing missiles with tube-launched constraints. Their use has been limited, partly because they induce unique aerodynamic rolling moment and side forces, and they have been observed to cause a reversal in roll moment direction at transonic speeds for unguided direct fire type missiles. Prior available information has been insufficient for the missile designers to make accurate estimates of roll moment coefficients for missiles with WAF. It has generally been assumed that the aerodynamic static stability could be estimated from a planar fin with a planform area equal to the projected area of the WAF, but this has not been demonstrated by making comparisons under controlled testing.

Because of the continued interest in tube launched missiles, a need exists to adequately define the parameters that influence the aerodynamic behavior of WAF by a systematic parametric approach. This report presents a summary of the results accumulated from a series of wind tunnel tests designed to study various parameters of WAF. An attempt has been made to obtain data for the purpose of defining the importance of each parameter on the aerodynamic rolling moment and side force induced by WAF, and provide the aerodynamic designer adequate information for preliminary estimates of rolling moment coefficient induced by WAF.

2. Discussion of Test Conducted and Model

Wind tunnel tests were conducted at two facilities. Transonic tests were conducted at the AEDC-PWT 4-foot tunnel [1, 2, 3], and the supersonic test at the Langley UPWT 4-foot section number 1 [4].

The angles of attack were varied between -6 and 6 degrees. Mach numbers were from 0.3 to 2.86 for several configurations. Roll angles were varied by rolling the model, balance, and sting with a remote roll mechanism. A complete matrix of configurations tested is contained in Table 1.

The model was supported by a 6-component strain gauge force balance, and each fin was instrumented with a 3-component force balance [1, 2, 3, 4].

The models consisted of a 2-caliber secant ogive nose with an 8-caliber cylindrical afterbody with three afterbody shapes and sixteen fin configurations. The basic body configuration had a straight cylindrical afterbody, 4 inches in diameter, and two alternate afterbody shapes stepped down to a diameter of 3.6 inches over a length of 7 and 4 inches, respectively, from the base (Figure 1).

The exposed semi-span $b/2$ for the WAF was chosen to be approximately the chord length for the arc that encloses a quadrant of tubular body cross section, or $0.707 D$. This description is shown in Figure 2, and the complete fin dimensions are given in Table 2. The exposed semi-span, therefore, was approximately the same, 2.658 inches for all fins. Aspect ratio for fins with unswept leading edge then was varied simply by changing the chord length. The geometric parameters varied are: 3 chord lengths (rectangular planforms), 4 leading edge shapes, 3 thickness variations, 4 leading edge sweep angles, 1 fin body gap, 1 tip chord alteration, and several fins tested on the stepdown body configurations. Figure 3 shows the WAF model in the AEDC 4T wind tunnel test section, and Figure 4 shows the fins tested.

3. Comparison of WAF to Flat Fin Stability and Drag

The major concern of the effects of WAF has been the self induced rolling moment; however, a comparison of static stability parameters was made for a flat fin and WAF. The flat fin had the same total exposed span and projected area as the WAF. These two fins were tested through the Mach number range of 0.3 to 2.86 on a body of revolution. The normal force coefficient slope at zero angle of attack and the center of pressure are shown in Figure 5 for both the flat fin and WAF. Any difference on total configuration static stability coefficients appears to be within the uncertainty of measurement accuracy.

The flat fin and WAF were also compared by testing both on a splitter plate (Figure 3) at transonic speeds. Figure 6 shows the flat and WAF basic fin lift curve slope at zero angle of attack along with the longitudinal and lateral center of pressure for the fin on a flat plate and on the body of revolution. The only significant difference between the splitter plate data and the data for fins on the body of revolution is the increase in normal force coefficient caused by body upwash. The upwash factor obtained from the ratio of these two curves ranges from 1.4 to 1.7 through the Mach range of 0.3 to 1.3. This is comparable to the slender body factor of 1.39 for this fin with a body diameter to total span ratio of 0.43.

The zero angle of attack forebody axial force coefficients for several of the geometric parameters tested are shown in Figure 7. The forebody axial force coefficient showing a comparison between the WAF, flat fin, and the body alone is included. The fin drag curve in Figure 5 is a comparison of the fin drag with the body alone subtracted out. The WAF is shown to be approximately 10 percent higher which corresponds to the additional frontal area that the WAF has due to the curvature.

The other geometric parameters (leading edge sweep, thickness, leading edge shape, and aspect ratio) show their influence on drag to be as expected for flat fins with the same shape changes.

4. Rolling Moment Coefficient

It appears from the previous section that the static stability derivatives are not significantly different for the flat and WAF. There is, however, a significant self induced roll moment produced by the WAF even at zero angle of attack. This missile rolling moment is the result of the normal force which the WAF induces at zero angle of attack that is not reflected in the stability gradients. The bias normal force is relatively small when only one panel is considered and for the data from the above test could not readily be isolated from other test anomalies such as tolerances in the angle-of-attack mechanism and fin cant.

The main objective for this study was to investigate the effects on rolling moment of the various geometric parameters of WAF. The variation of rolling moment is considered for three flow parameters: Mach number, Reynolds number, and angle of attack for several geometric variations. Featherstone [5] and others [6] have shown the WAF to have self induced normal forces at zero angle of attack. Figures 8 through 16 show the effects of the various fin geometric parameters on the zero angle-of-attack rolling moment coefficient for Mach numbers 0.3 to 2.86. The most significant effect with Mach number appears to be at transonic speeds where, in general, a change in sign occurs for rolling moment. Featherstone has suggested the self induced force is directed toward the center of curvature at subsonic speeds and away from the center of curvature at supersonic speeds with the cross over occurring close to $Mach = 1$. This was demonstrated for those fin configurations with a $C_{R/D} = 1.75$ with the exception of the fin with maximum thickness $t/C = 0.045$. This trend exists for fins with rectangular planform, those with leading edge sweep (Figure 10), on both straight and step-down body (Figure 12), for leading edge profile modification (Figure 8), and for modifications to both root chord gap fin and the tip chord (Figure 14).

a. Geometric Parameters

Two geometric parameters that show significant variations especially at higher Mach numbers are the unsymmetrical leading edge and the stepdown body. The majority of fins were tested with a 45-degree symmetrical leading edge wedge; however, four leading edge variations were made. The symmetrical leading edge wedge included angles tested at 45 degrees, 20 degrees, and blunt (Figure 2 and Table 2). The rolling moment coefficients are presented in Figure 8. Only the unsymmetrical leading edge shows significant effects on rolling moment. It

has little effect at low speeds; however, at supersonic speeds a large effect on rolling moment was observed. The 22.5-degree beveled leading edge is expected to act as a wedge in supersonic flow. The WAF leading edge wedge pressures are expected to have magnitudes somewhere between those on a two-dimensional and three-dimensional wedge perhaps closer to the values of the two-dimensional. For a two-dimensional 22.5-degree wedge the shock is not attached below approximately Mach 2.0, but the three-dimensional shock is attached at Mach 1.3. From Mach 1.0 to 1.3 the leading edge is behind a detached shock and is in subsonic flow, and between Mach 1.3 and 2.0 the leading edge could be exposed to mixed subsonic and supersonic flow. Beyond Mach 2.0 the shock is attached and the leading edge is exposed to full supersonic flow. These transient conditions in flow regime along with shock wave interaction with adjacent fins are most likely responsible for the large variations between Mach 1.1 and 2.0. An analytical method to predict or describe this trend is not available at this time.

Another geometric parameter that did show significant effect on WAF self induced zero angle-of-attack rolling moment was aspect ratio. The aspect ratio was changed by a change in root chord length for fins with unswept leading edges.

Figure 9 shows how aspect ratio effects the zero angle-of-attack rolling moment coefficient for fins with unswept leading edge. The higher aspect ratio appears to cause rolling moment to become more negative at low speeds, but at supersonic speeds the effect is insignificant over the range considered. Changing the aspect ratio by sweeping the leading edge did not show the differences (Figures 10 and 11) as the unswept case did (Figure 9). These trends indicate that an important parameter on the WAF self induced rolling moment at least for low speeds is the fin chord length at the body fin juncture. Also shown in Figure 11 is the effect of fin thickness on rolling moment for fins having $t/C = 0.015$, 0.03 , and 0.045 . The thickest fin ($t/C = 0.045$) shows some deviation from the other two which are near identical. A WAF of this type with $t/C = 0.045$ is a heavy structure and most probably would never be used. A t/C in the range of 0.015 to 0.03 is more reasonable, and for this spread it does not appear that the WAF self induced rolling moment is affected by thickness.

The remaining geometric parameter investigated was the step down body (Figures 12 and 13). The body step down equal to the thickness of the 3 percent fin with a $C_R/D = 1.75$. The only significant difference noted for the step down body occurs in the supersonic range, where the step down tends to cause a positive shift in roll moment coefficient.

b. Flow Parameters

Reynolds number (Figures 15 and 16) did not show any significant alteration of the rolling moment sign reversal at transonic speeds for the range 2 to 5 million per foot.

The variation of rolling moment coefficient with angle of attack for several representative configurations are shown in Figures 17 through 22. Figure 17 shows that the flat fin has small change with angle of attack throughout the Mach number range; however, the WAF (Figures 18 through 22) configurations show a distinctive rolling moment coefficient variation with angle of attack. The rolling moment coefficient remains fairly constant over an angle of attack, α , range of -2.0 to 2.0 degrees. For the lower Mach numbers through the transonic range the rolling moment generally becomes more positive at -2 degrees $> \alpha > 2$ degrees, and for the supersonic Mach numbers the rolling moment decreases at -2 $> \alpha > 2$. This trend is typical and is shown for three aspect ratios (Figures 18 through 20), two leading edge shape variations (Figures 18 and 21), and two leading edge sweep angles (Figures 18 and 22).

The data presented herein show that while the variation of rolling moment coefficient with Mach number can be significant, only small changes occur for 2 degrees $> \alpha > -2$ degrees. Many tube launched missiles equipped with WAF fly direct fire type trajectories where the angle of attack envelope is well within ± 2 degrees. Flight simulations can be simplified to use only the zero angle-of-attack self induced rolling moment coefficient.

5. Accuracy of Rolling Moment Coefficient Data

Some questions have arisen concerning the accuracy and repeatability of the rolling moment coefficient data. The magnitudes of the self induced rolling moment coefficients of the WAF are quite small relative to the size of coefficients of fins with large cants. The only ready means of obtaining force data in a wind tunnel is with a strain gauge balance. The balance must be sized to meet special requirements, but it must be capable of handling the forces and moments of the complete model in the test facility to be used. To obtain sensible rolling moment coefficients induced by WAF, both wind tunnel dynamic pressure and fin sizes must be made large within practicable limits. Both cause larger aerodynamic loads on the model which results in requirements of larger strain gauge balances. To date strain gauge balances are not ideal for measurement of these small rolling moments; however, from the available balances one can be chosen that is optimum for given requirements. A composite plot of rolling moment data precision is shown in Figure 23. At transonic speeds the rolling moment gauge was large because of the requirements dictated by normal force and pitching moment loads. As a result the data precision, as quoted by Arnold Engineering Development Center (AEDC) [1, 2, 3] are larger than desirable; however, as shown later the repeatability from duplicate points during the same test and from separate entries show that the data are reproducible well within these precision limits. An attempt was made to measure the cant of each fin during the transonic testing [1, 2]. These measurements of 76 fin installations had a mean cant of

0.011 degree with a standard deviation of 0.142 degree, with a quoted measurement accuracy of ± 0.1 degree. If all four fins for one configuration have a 0.1-degree cant, the rolling moment coefficient would be 0.004 to 0.006 which is well within the quoted (Figure 23) data precision for the transonic test and just slightly above the data precision for the supersonic test. Because of the uncertainty of the cant measurements and the small magnitude of fin cant induced rolling moment relative to the data precision, corrections to rolling moment coefficient caused by fin cant are not presented.

Comparisons are made from the numerous duplications and other geometric similarities. From these one can decide where these results can be beneficial in making predictions of the WAF self induced rolling moment. Several specific cases where comparisons are made are as follows:

a) Direct reruns - A separate test [3] was conducted explicitly to check rolling moment obtained in earlier test [1] at transonic speeds. This test was conducted with a balance that had a 100-inch-pound roll moment gauge. The normal force and pitching moment gauges were also low capacity and angle of attack was restricted to less than 2 degrees. The quoted data precision for the rolling moment coefficient is shown in Figure 23, indicated by the AEDC report [3]. The main purpose of this test was to observe the self induced WAF rolling moment coefficient at zero angle of attack, and compare these to previously obtained coefficients with the less sensitive balance. Comparisons of three configurations are shown in Figure 24.

b) Roll angle - The models were tested at 0- and 45-degree roll angles (Figure 1) throughout the Mach number range at angles of attack of -6.0 to 6.0 degrees. The outcome of the rolling moment coefficient should be the same for any roll angle at zero angle of attack from a flow and model symmetry viewpoint. Differences between roll position can be attributed to data instrumentation repeatability. Figures 25 and 26 show self induced WAF rolling moment coefficients at zero angle of attack throughout the Mach number range for two roll angles of 0 and 45 degrees. This does not necessarily indicate the precision of the data, but these results are typical of the repeatability of the data for both the transonic and supersonic phases of testing. Tests were conducted for other roll angles during the transonic phase, and all results were compatible with those shown in Figures 25 and 26.

c) Computed roll moment from fins - Each fin was mounted on a 3-component strain gauge balance. These balances were designed to accommodate the loads experienced during the transonic testing, but were used also for the supersonic test where the loads were far below the design maximum. Total missile rolling moment coefficient was computed from the measured fin normal force and root bending moment coefficient and compared to the rolling moment coefficient obtained from the main balance. Typical comparisons of the WAF self induced rolling moment coefficient at zero angle of attack for the transonic test are shown in

Figures 26 and 27. Fin data exist for the supersonic phase and are adequate for obtaining the usual normal force coefficients for stability considerations, but data scatter prohibits a meaningful computation of total missile rolling moment coefficient for angles of attack near zero. The data most questionable are the transonic phase, as shown in Figure 23 [1, 2], where comparison between the two methods of obtaining rolling moment coefficient are better than expected.

As usual in experimental data there are some cases where results do not reach desired quality; however, the data presented in this report are believed to give one a basic knowledge of the characteristics of the WAF for several of the geometric and flow properties.

6. Side Forces and Moments

It has been suggested [6] that in addition to inducing rolling moments, the WAF causes side force and moment variations with pitch angle of attack. Nothing was observed during this series of testing that substantiate the generation of cross derivatives of significant magnitude over the angle of attack range ± 6 degrees for standard opening direction and angles. Figures 28 through 33 present a sample of typical side force variation with angle of attack for the flat fin, and several of the geometric changes made of the WAF. Figure 28 shows the side force coefficient variation with angle of attack for the flat fin, and Figure 29 shows the WAF with identical projected planform area and profile to the flat fin. It can be seen that very little difference exists between the two and that essentially no side force change with angle of attack occurs for the WAF. The small bias shown can easily be due to wind tunnel flow and model misalignments, and are present in all configurations. The yawing moment is not shown, but similarly the moment remains constant throughout the angle-of-attack range tested. Side forces are shown for the three aspect ratio variations for the WAF with rectangular planforms tested in Figures 29, 30, and 31. Figures 32 and 33 show that neither the unsymmetrical leading edge or leading edge sweep on the WAF cause aerodynamic cross derivatives below 6 degrees angle of attack. These are all shown at a roll angle with the fins vertical and horizontal ($\phi = 0$) or in the + configuration. The model was tested at roll angles of 22.5 and 45 degrees (Figure 1), and side forces and moments were not observed to change for any of these cases at any Mach number below 2.86.

7. Typical Missile Roll Rate with WAF

The unusual roll rate behavior of wrap-around finned missiles during flight has been observed among missile designers since the inception of the WAF. This report has shown data substantiating that the WAF induces a roll moment coefficient even at zero fin cant; however, the magnitude of these roll moments appear to be small, and it has

been difficult to measure them by conventional wind tunnel testing. The reason that these small moments cause roll rate variations in flight to be conspicuous is that missiles typically also have small mass moments of inertia in roll.

To illustrate the effects during flight of the zero lift rolling moment coefficients of missiles with WAF, several comparisons between the roll effectiveness of flat fins and WAF were made. A computer program written for the purpose of obtaining roll rate information was used. Trajectory data (Mach number and altitude versus time) and roll mass moment of inertia for a typical missile were used as inputs. The Mach number ranged from 0.0 to 3.0, and the roll moment of inertia ranged from 0.2 at motor ignition to 0.14 lb-ft-sec^2 at motor burnout ($M = 3.0$). The aerodynamic inputs are restricted to the roll moment coefficient due to cant, the roll damping coefficient and the self induced WAF rolling moment. The only assumption is that these three roll moments can be combined linearly. Figure 34 shows the roll rate variation for the flat fin case with an initial roll rate of 10.0 cps at three fin cant angles of -1.0, 0.0, and 1.0 degrees. Figure 35 shows the same except the self induced roll moment coefficient for the WAF has been included. It can be seen that the effects of the WAF self induced roll moment is approximately equal to the effects of rolling moment due to a 1.0-degree cant at the higher Mach numbers.

A recent test has been conducted where an attempt was made to obtain roll damping for several fin configurations. Included in this was a comparison between a flat fin (F9) and a WAF (F1, see Figure 2 and Table 2). These data have not been published at this time. The model was spun up in the wind tunnel by an internal hydraulic motor. At a prescribed roll rate the motor clutch was released and the model was allowed to free spin until the steady state roll rate was reached. Figure 36 shows the measured steady state roll rate for the WAF with fin cant angles of 0 and 1 degree at Mach numbers from 0.3 to 1.3. A comparison of the flat fin and WAF is shown for the 1 degree cant. The roll rate for the flat fin and WAF remains approximately the same through Mach number 0.8. Above Mach 0.8 the WAF deviated sharply away decreasing until at Mach 1.3 the roll rate was essentially zero. Thus the free spinning results substantiate the abrupt negative shift in rolling moment shown by the static data (Figure 8).

8. Conclusions

The general characteristics of a number of WAF on a body of revolution at Mach numbers 0.3 to 2.86 have been presented. The effects of geometric and flow parameters have led to the following conclusions:

- a) The static stability derivatives at $\alpha = 0$ of missiles with WAF are essentially the same as with equivalent planar fins and may be estimated by using the flat fin techniques.

b) Drag of the WAF is larger than the flat fin with the same projected planform area. This increase is approximately a factor of 1.1, for the fins tested, which corresponds to the increase in frontal area of the WAF over the flat fin.

c) The WAF does induce roll moment to the missile at zero angle of attack and zero fin cant.

d) The WAF self induced roll moment can change direction as a function of Mach number, with the cross over occurring near Mach 1.0. The resulting moment direction is determined by the fin force directed toward the fin center of curvature at subsonic speeds and away from the center of curvature at supersonic speeds.

e) The WAF rolling moment variation with total missile angle of attack is small for absolute angles of attack less than 2 degrees. Above 2 degrees the rolling moment may deviate significantly from the zero angle of attack case depending upon fin geometry and Mach number.

f) Cross derivatives induced by the WAF do not appear to be significant at any Mach number below an angle of attack of 6 degrees. This may not be the case for WAF configurations where fin opening directions are alternated, or for higher angles of attack.

g) Accurate measurement of WAF rolling moment requires sensitive roll moment measurement instrumentation, and small tolerance on the individual fin geometric incidence.

h) The WAF moments do not appear to be intolerable, and missile roll rates can be tailored by proper geometric design and fin incidence for many applications.

TABLE 1. SUMMARY OF WAF TEST

Configuration	Mach No.													
	0.30	0.50	0.80	0.95	1.00	1.05	1.10	1.20	1.30	1.60	1.90	2.36	2.86	
B1	●	○	●	●	●	○	●	○	●	◇	◇	◇	◇	
B1F1	●▲	○▲■	○▲■	○▲■	○▲■	○▲	○▲■	○	○▲■	◇	◇	◇	◇	
B1F2	●▲	○▲	○▲	●▲	●▲	○▲	●▲	○▲	○▲	◇	◇	◇	◇	
B1F3	●▲	●▲■	●▲■	●▲■	●	○▲	●▲■	○▲■	●▲■					
B1F4		○	○	○	○	○	○		○					
B1F5		○	○	○	○	○	○	●	○					
B1F6		○	○	○	○	○	○	●	○	◇	◇	◇	◇	
B1F7	▲	○▲	○▲	○▲	▲	○▲	○▲	○▲	○▲	◇	◇	◇	◇	
B1F8	▲	○▲	○▲	○▲	▲	○▲	○▲	▲	○▲					
B1F9	○	○	○	○	○	○	○	○	○	◇	◇	◇	◇	
B1F10	○	○	○	○	○	○	○		○					
B1F11		○	○	○	○	○	○	○	○					
B1F12		■	□	□	□		□	□	□					
B1F13		□	■	■	□		□	□	■	◇	◇	◇	◇	
B1F14		■	■	■	■		■	■	■					
B1F15		■	■	■	■		■	■	■					
B1F16		□	■	■	□		□	□	■	◇	◇	◇	◇	
B2		●	●	●		●	●	●	●					
B2F1		○	○	○	○	○	○	○	○	◇	◇	◇	◇	
B2F9		○	○	○	○	○	○	○	○					
B2F10	○	○	○	○	○	○	○	○	○					
B2F13		□	■	■	□		□	□	■	◇	◇	◇	◇	
13F2		■	■	■	■	■	■	■	■					
B3F16		□	■	■	□		□	□	■					

○ Reference [1]
 △ Reference [3] Solid symbols - zero roll angle only
 □ Reference [2] Open symbols - 0, 22.5 deg and/or 45 deg roll angle
 ◇ Reference [4]

TABLE 2. FIN CONFIGURATION SUMMARY*

Configuration	A (in.)	C _R (in.)	C _T /C _R	Γ [*] (deg)	τ (in.)	R ₁ (in.)	R ₂ (in.)	R ₃ (in.)	δ** (deg)	r (in.)	AR
F ₁	1.900	7.0	1.00	0	0.200	1.900	2.000	1.800	45	0.008	0.75
F ₂		4.0			0.114		1.957	1.843	①		1.30
F ₃		2.0			0.057		1.929	1.871			2.60
F ₄		7.0			0.200		2.000	1.8000	20		0.76
F ₅									②		0.76
F ₆					0.107		1.953	1.847	45		0.76
F ₇					0.315		2.058	1.743			0.76
F ₈					0.200	③					0.75
F ₉	2.000					1.900	2.000	1.800			
F ₁₀ ④	1.900										
F ₁₁	Fin "7" with tip chord modified										
F ₁₂	1.9	7.0	0.9	14.75	0.200	1.9	2.0	1.8	45		0.73
F ₁₃			0.75	33.9							0.79
F ₁₄			0.60	46.9							0.86
F ₁₅		4.0	1.00	0	0.040	1.880	1.900	1.860			0.94
F ₁₆	1.9	4.0	0.75	20.05	0.114	1.9	1.957	1.843			1.28
											1.54

*See Figure 2 for definition of terms.

**Leading edge angle. All trailing edges δ = 45 deg.

① Blunt leading edge.

② Unsymmetrical leading edge.

③ Rectangular flat planform, exposed span = 2.658 in.

④ Gap fin.

⑤ Tip chord parallel to root chord

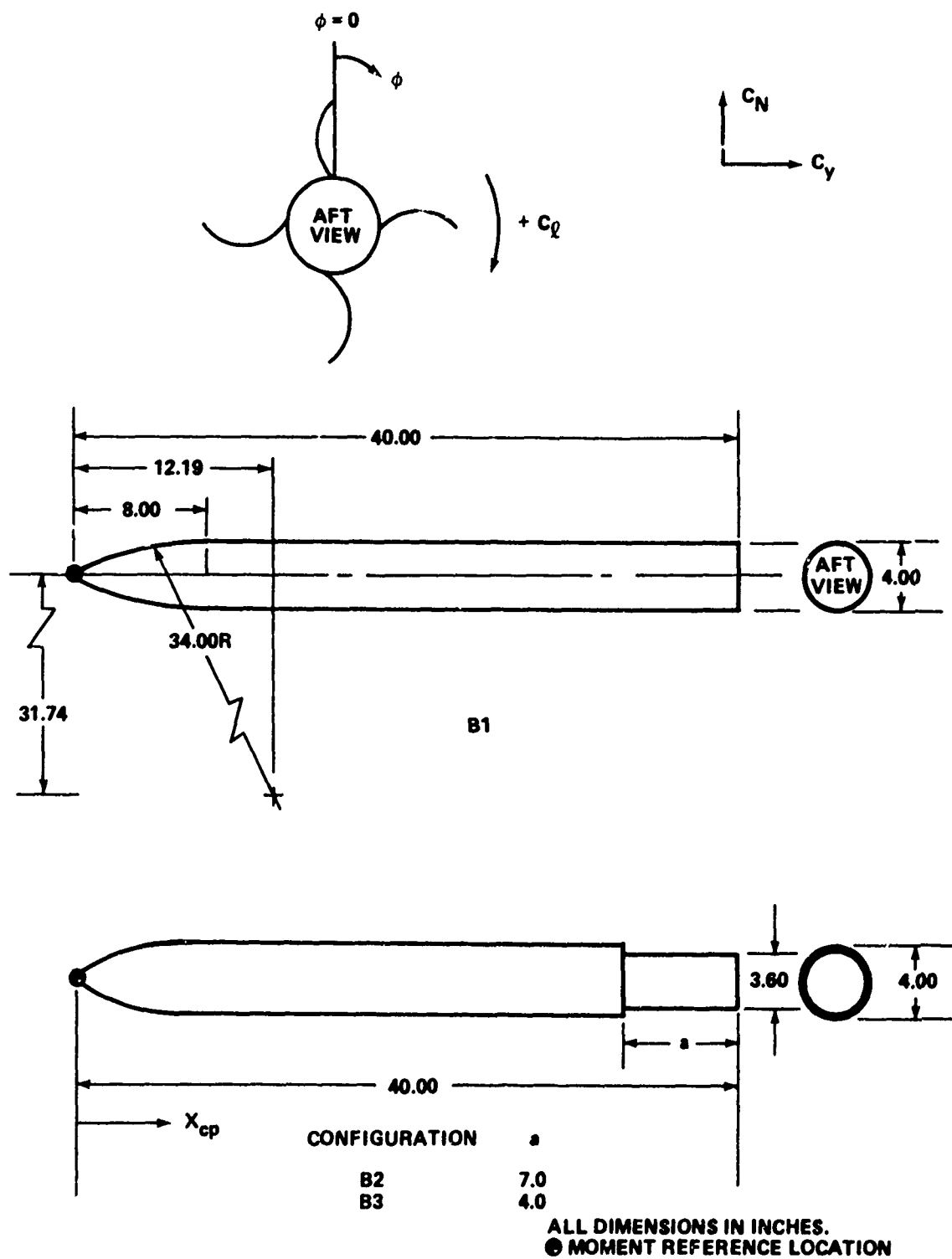


Figure 1. External body geometry.

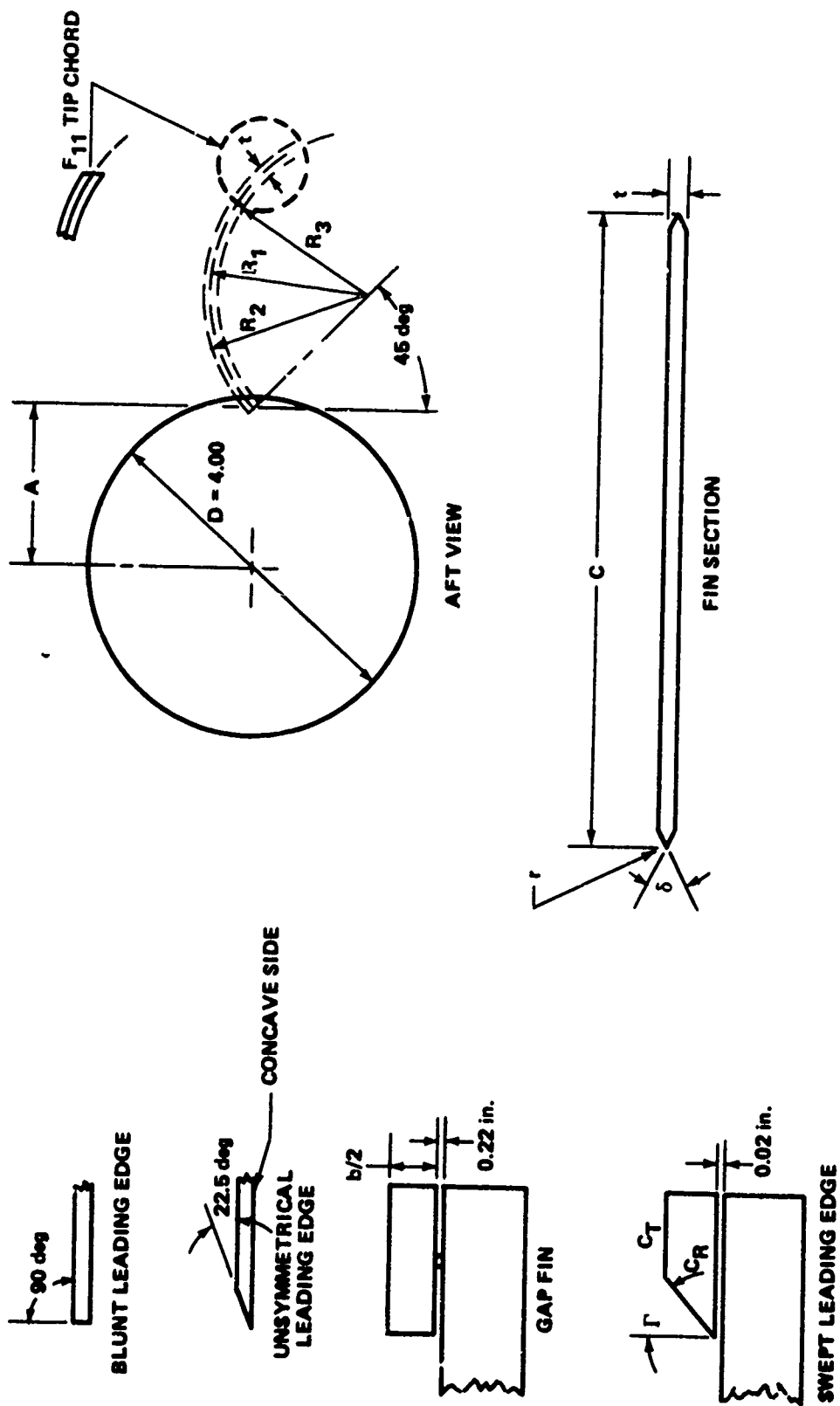


Figure 2. WAF geometry.



MODEL INSTALLATION STANDARD CONFIGURATION, $\phi = 0, \alpha = 0$



SWEPT FIN CONFIGURATION



SPLITTER PLATE

Figure 3. WAF model.

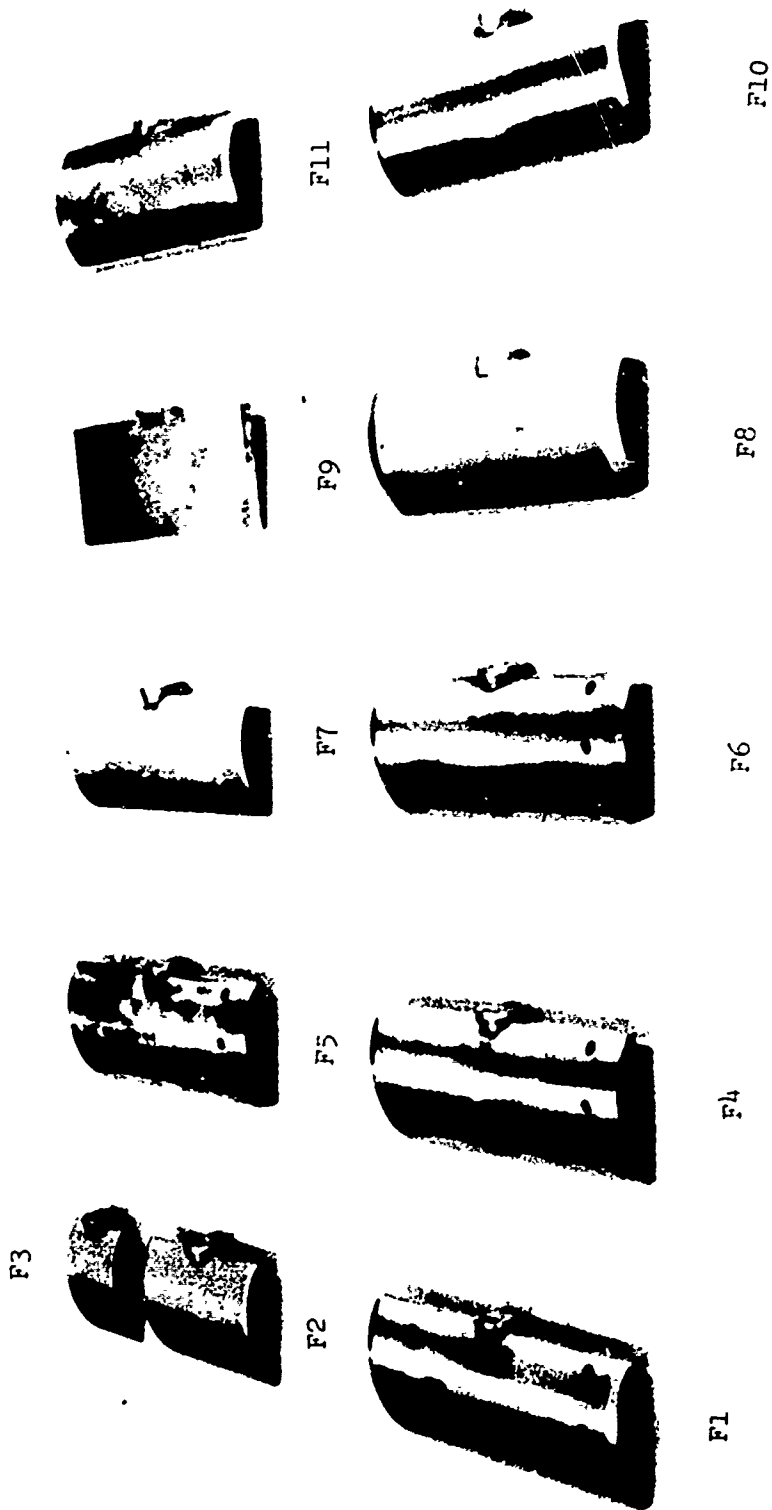
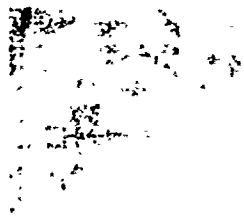


Figure 4. WAF.



F16

...

foot



F15



F14



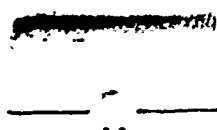
F13



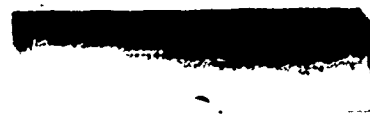
F12



F3



F2



F1



Figure 4. Concluded.

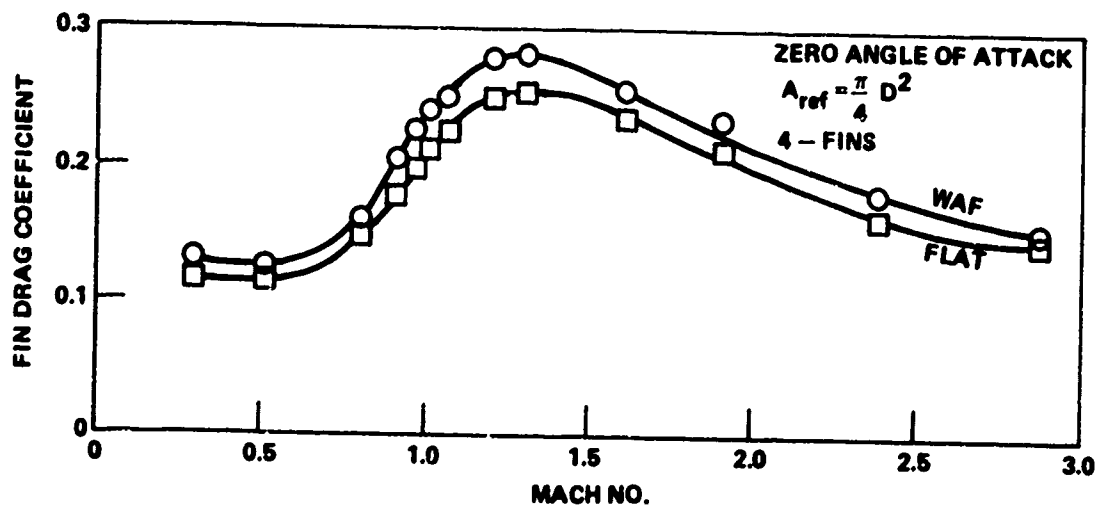
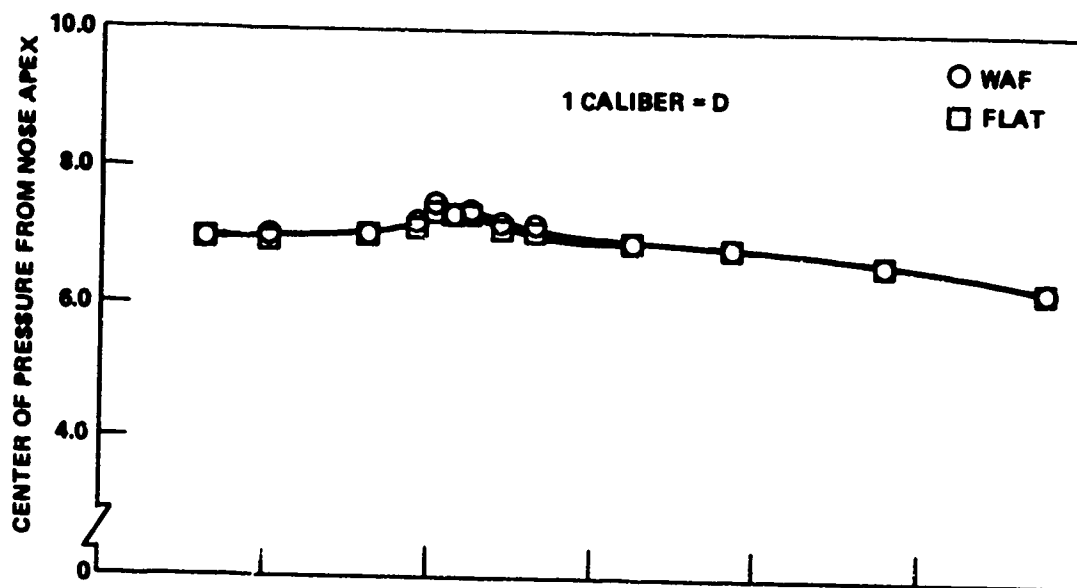
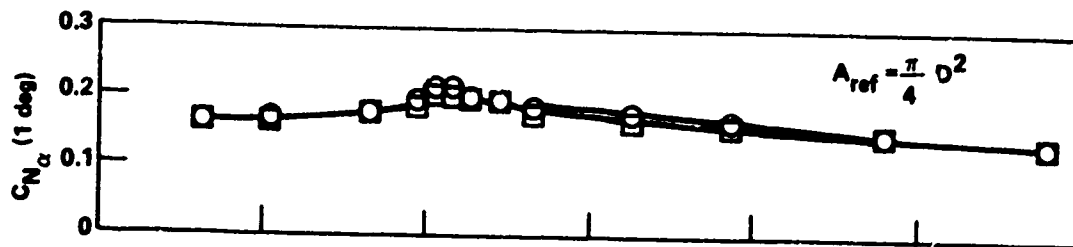


Figure 5. Comparison of WAF to flat fin static stability and fin drag coefficients.

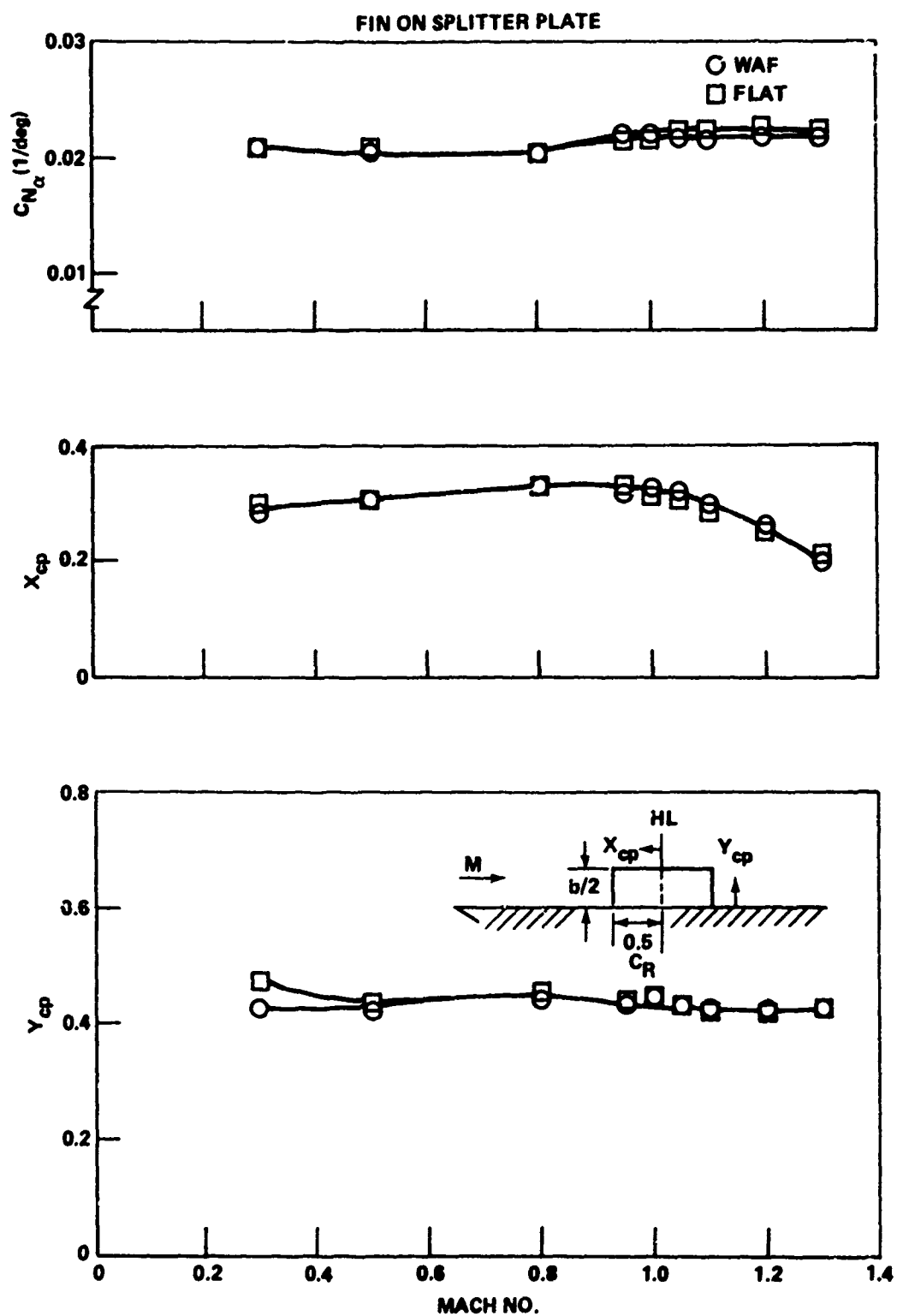


Figure 6. Comparison of WAF fin panel to flat fin panel static stability.

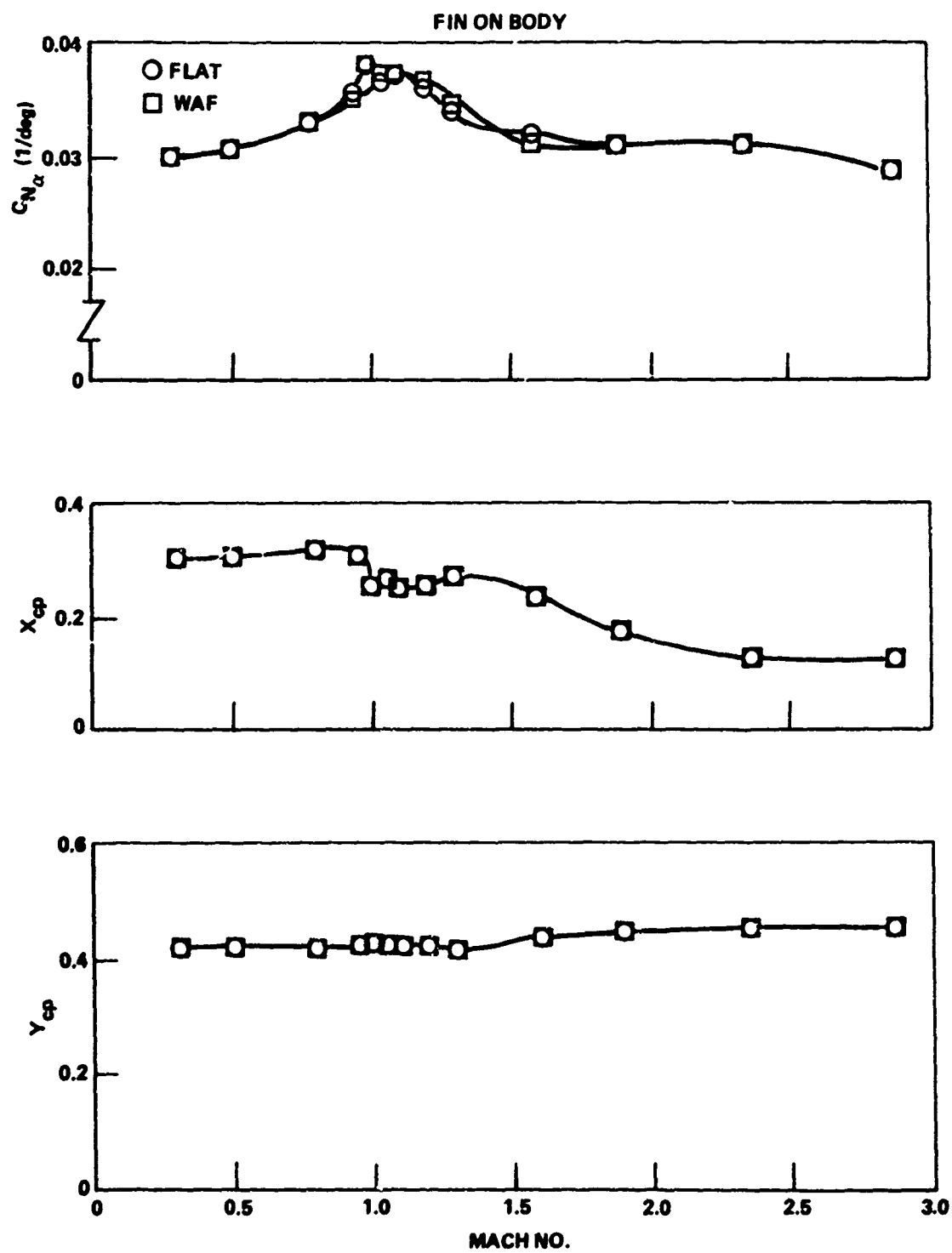


Figure 6. Concluded.

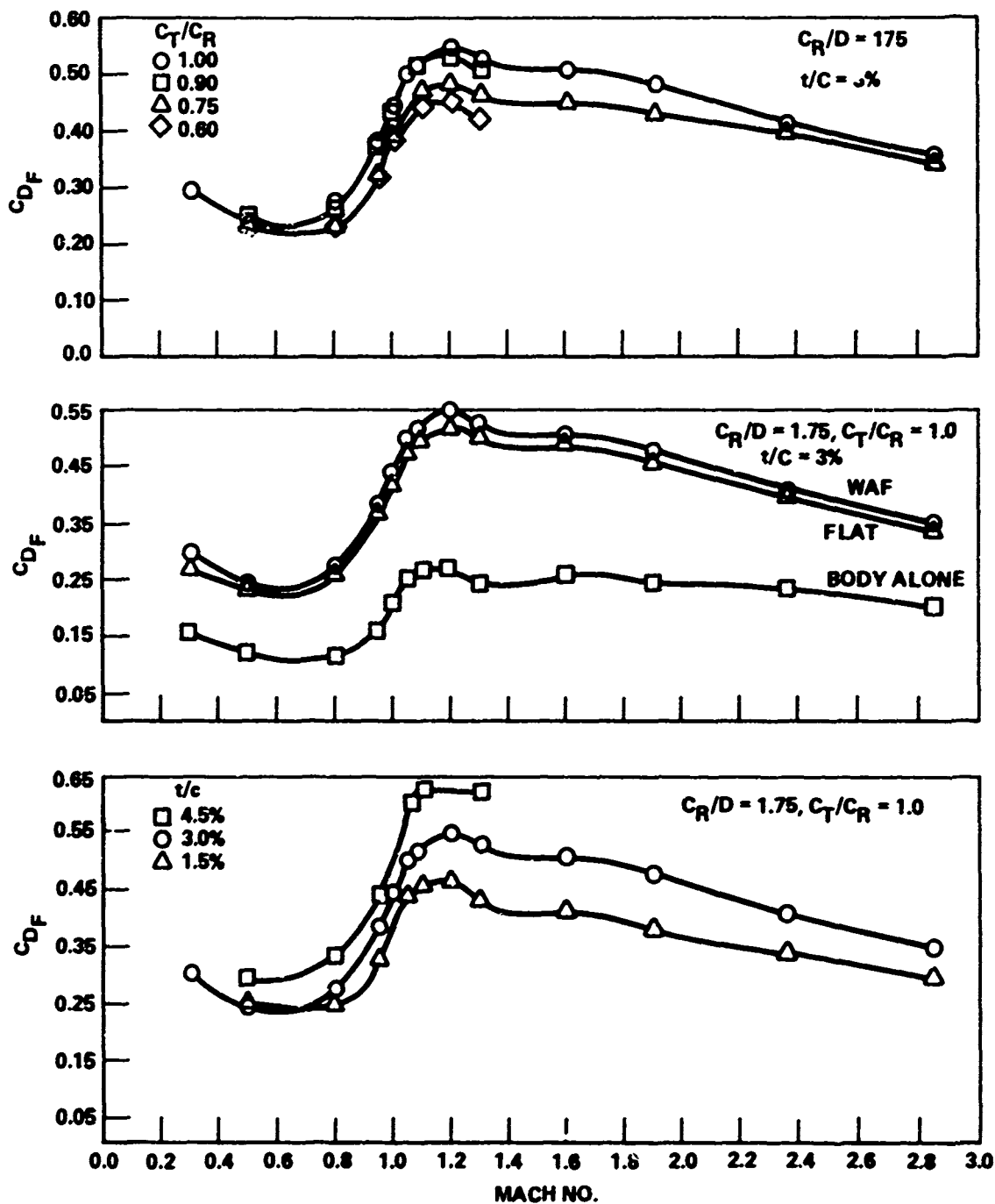


Figure 7. Effects of WAF geometric parameters on drag coefficient, $\phi = 0$, $\alpha = 0$.

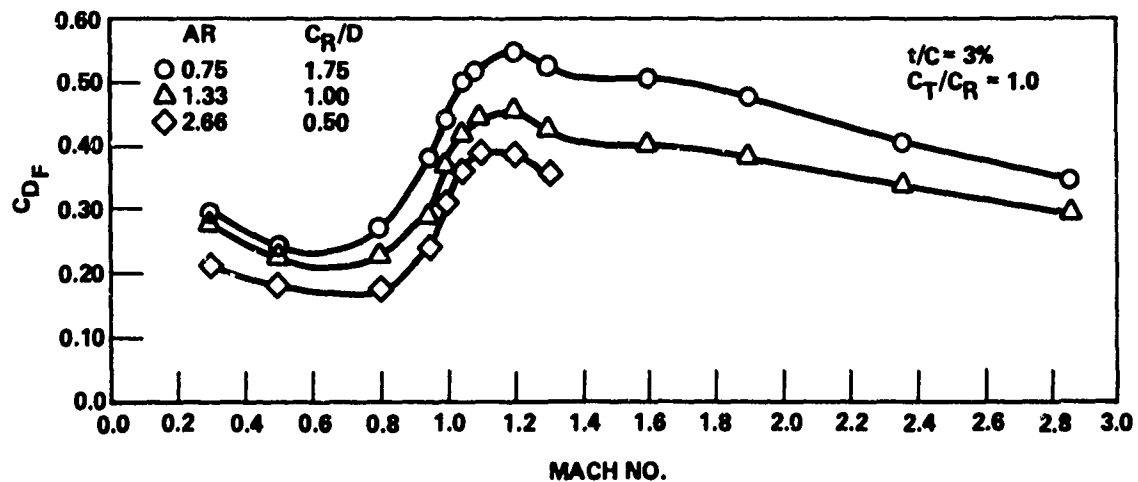
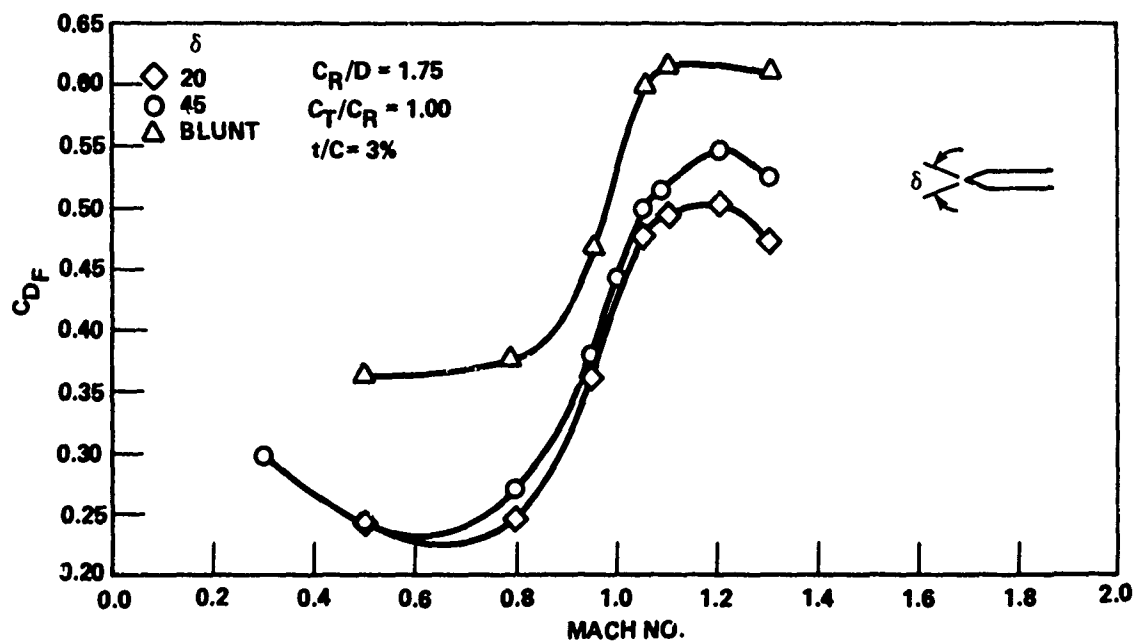


Figure 7. Concluded.

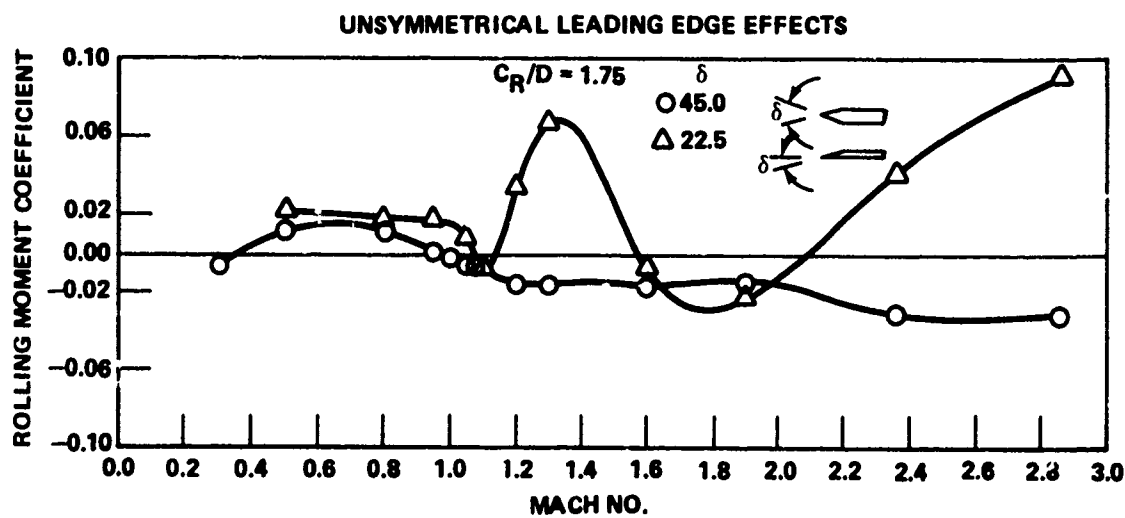
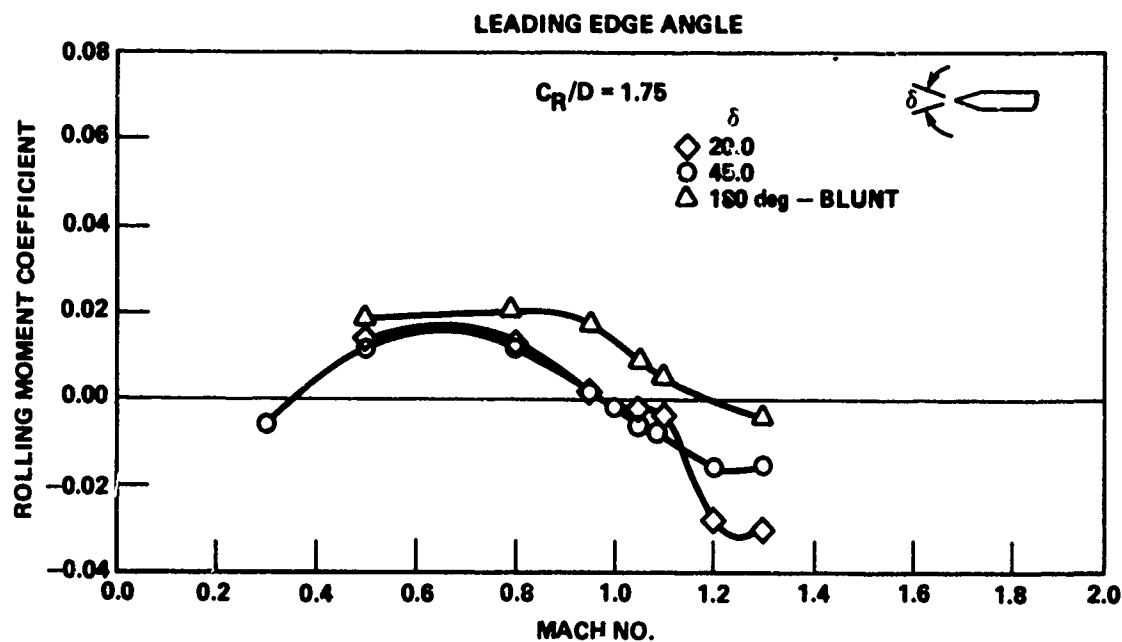


Figure 8. Effect of leading edge shape on WAF rolling moment, $\alpha = 0$, $t/C_R = 3$ percent.

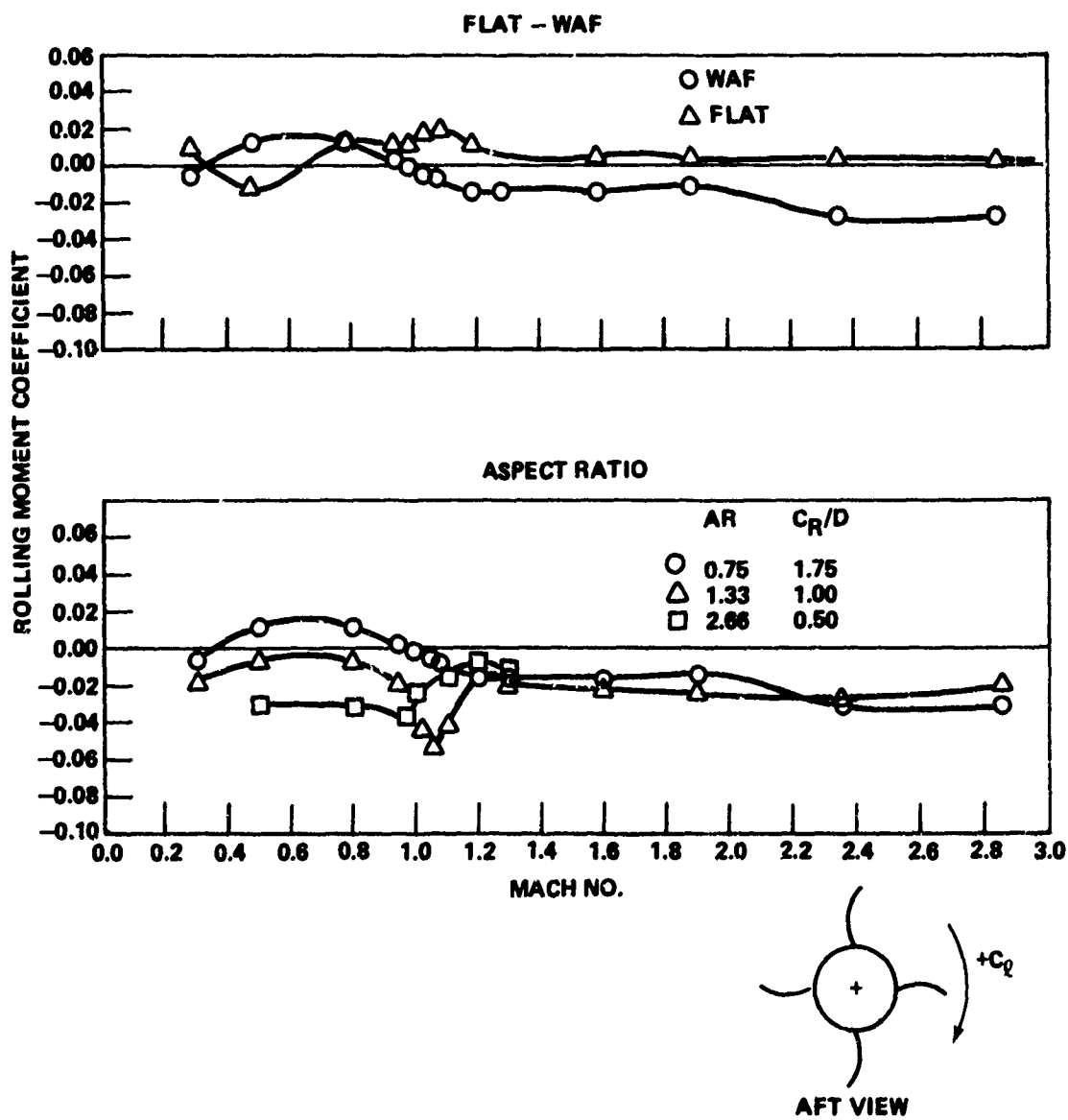


Figure 9. WAF rolling moment coefficient versus Mach No.,
 $\alpha = 0$, $t/C_R = 3$ percent.

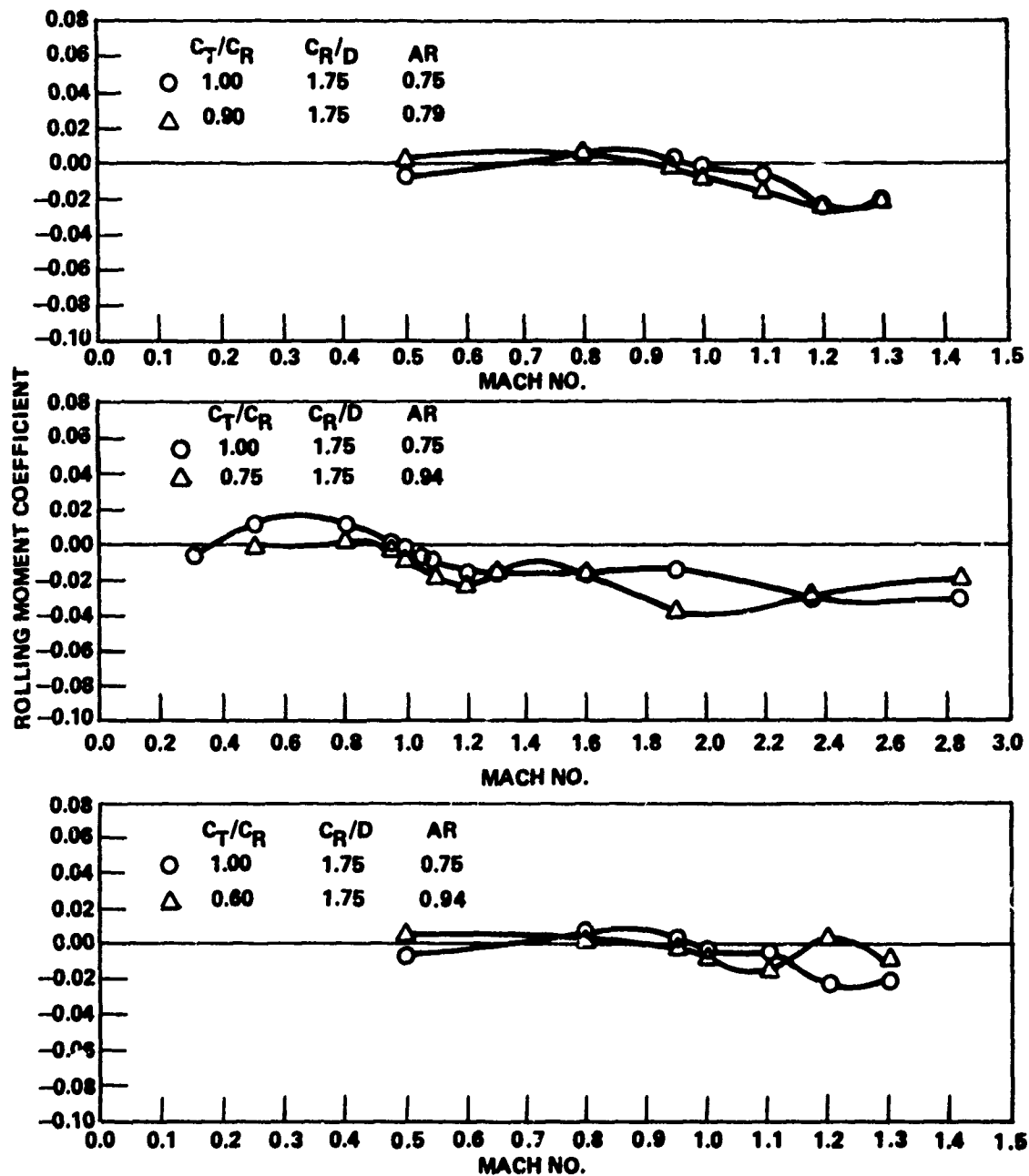


Figure 10. Effect of fin leading edge sweep angle on WAF rolling moment, $\alpha = 0$, $t/C_R = 3$ percent.

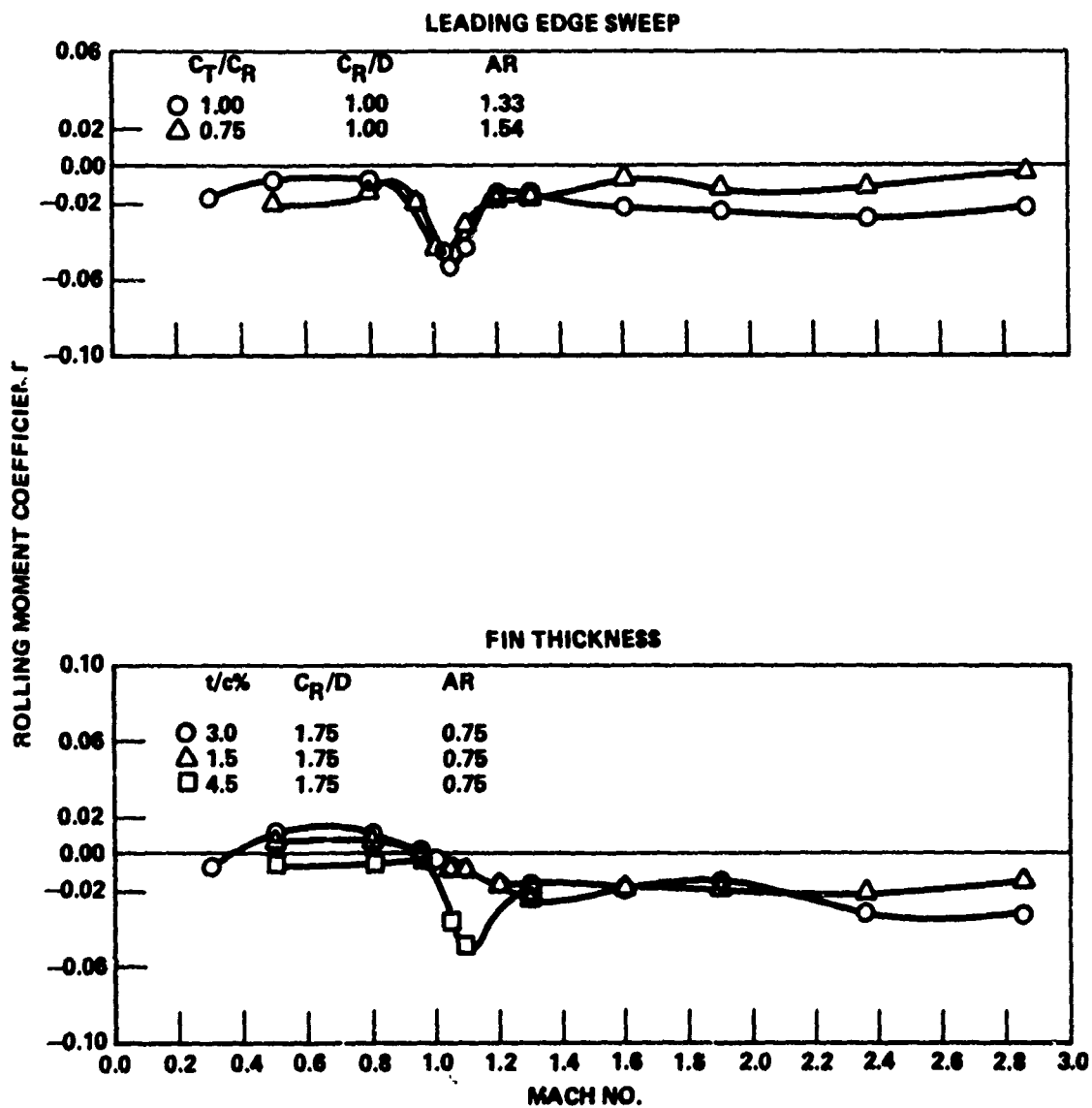


Figure 11. Effect of fin leading edge sweep and thickness on WAF rolling moment coefficient, $\alpha = 0$, $t/C_R = 3$ percent.

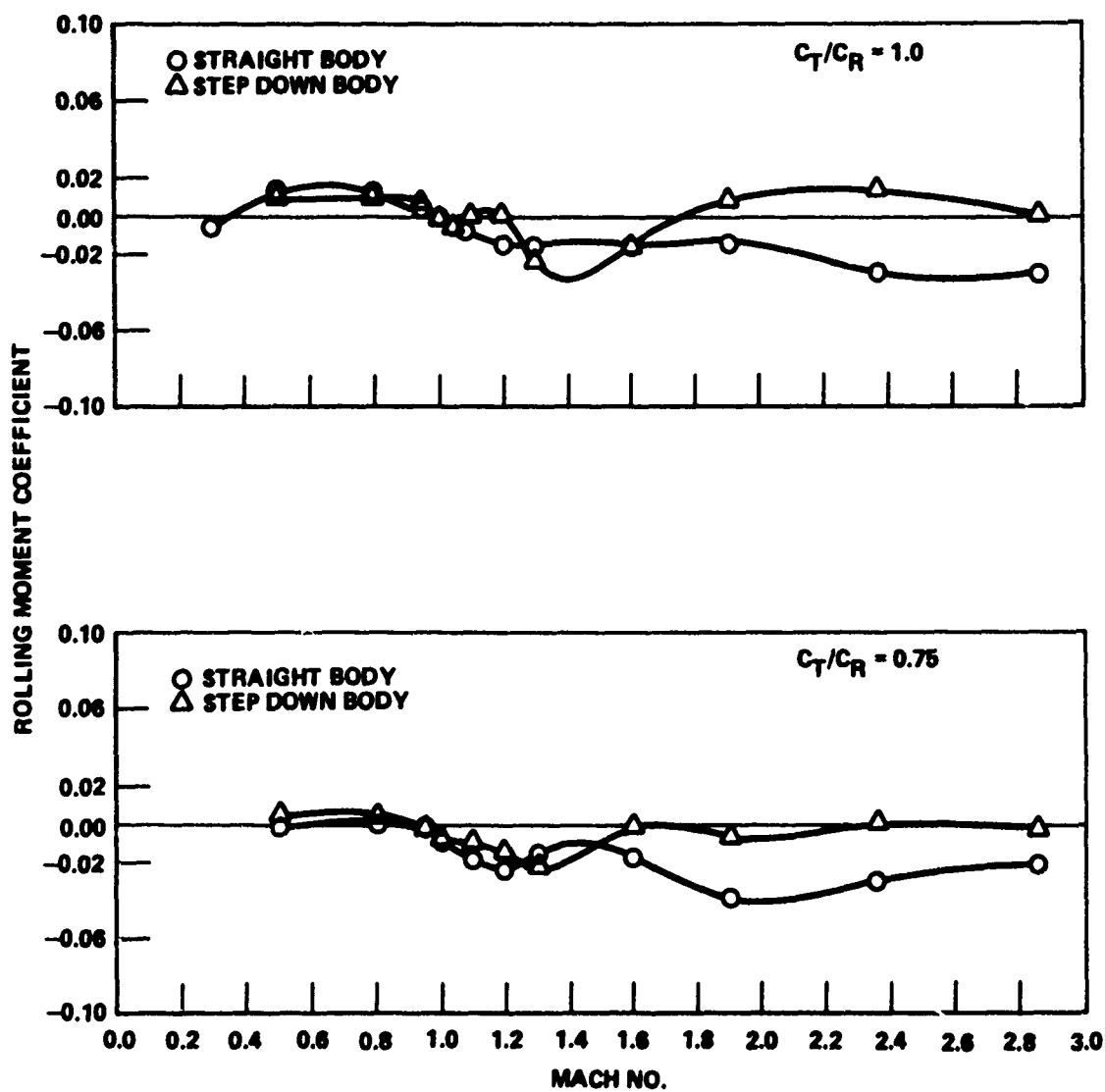


Figure 12. Effect of stepdown body on WAF rolling moment coefficient, $\alpha = 0$, $t/C_R = 3$ percent $C_R/D = 1.75$.

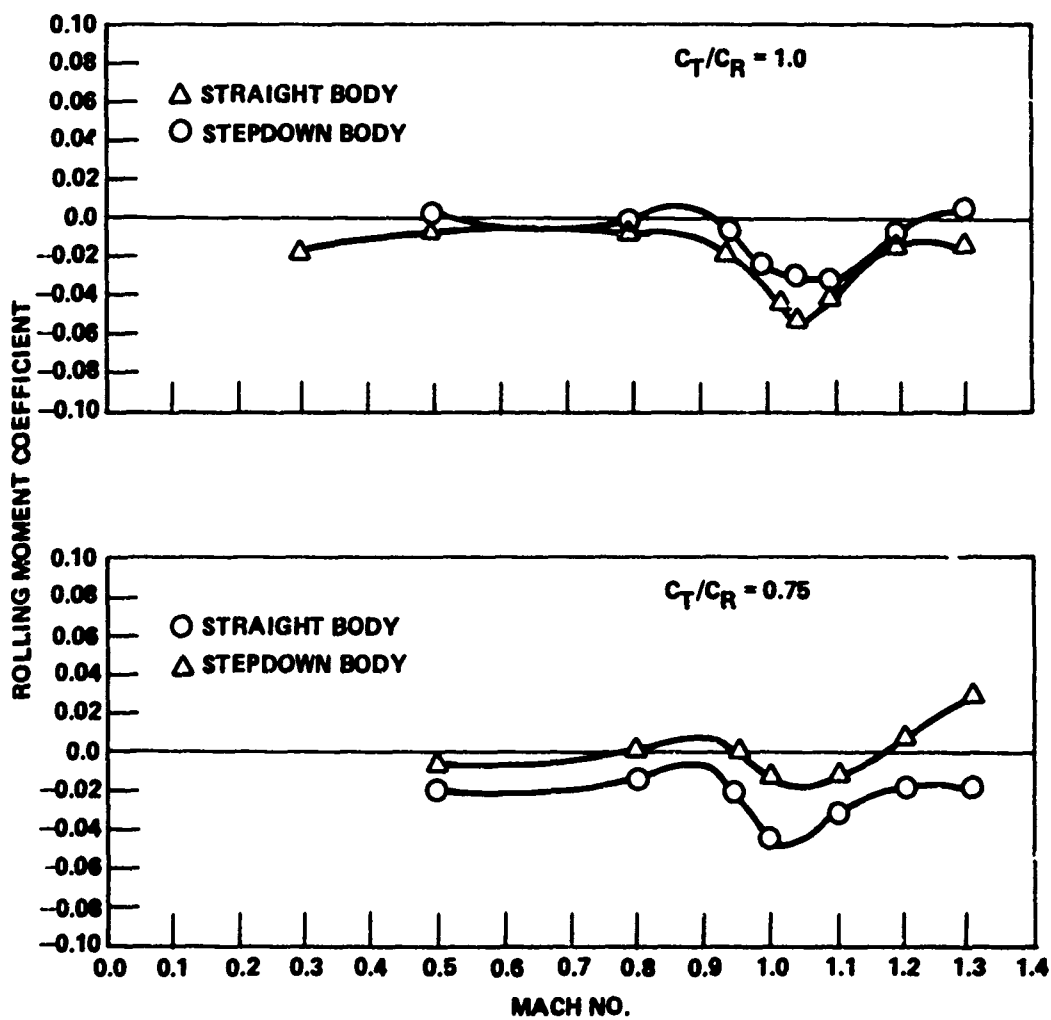


Figure 13. Effect of stepdown body on WAF rolling moment coefficient, $\alpha = 0$, $t/C_R = 3$ percent $C_R/D = 1.00$.

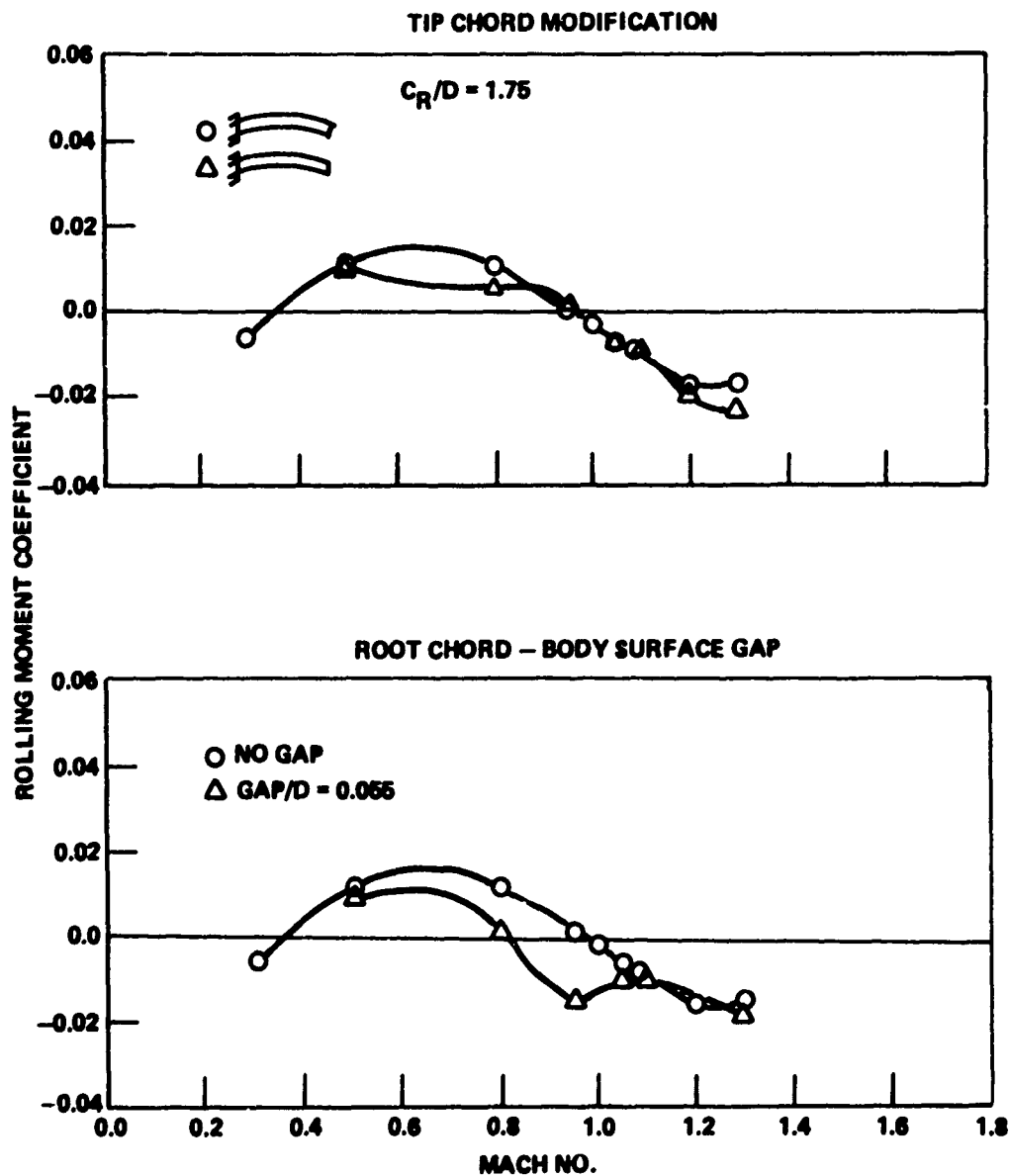


Figure 14. Effect of modifying WAF root and tip chord cross section on rolling moment, $\alpha = 0$, $t/C = 3$ percent.

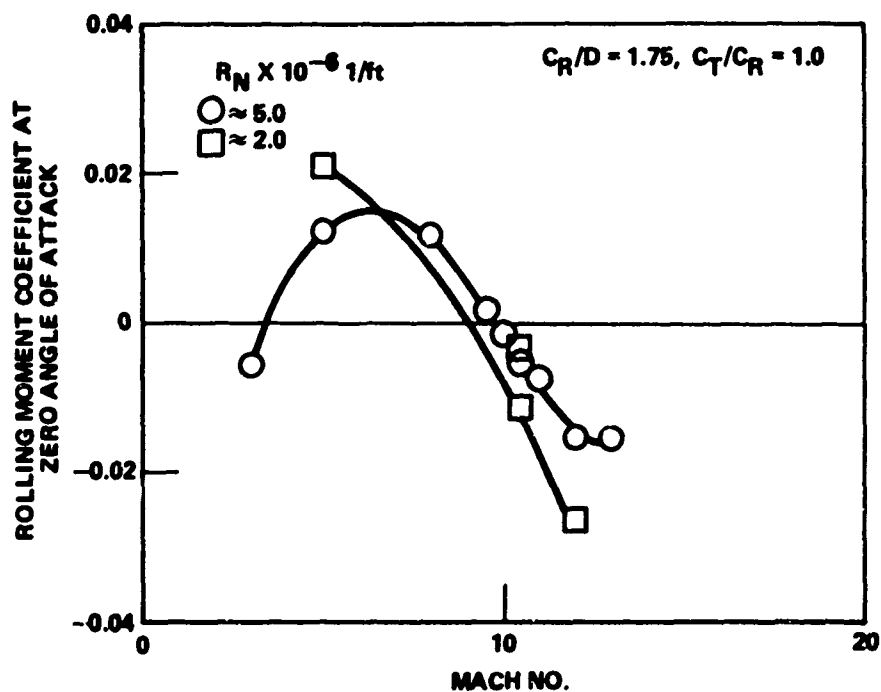


Figure 15. Effect of Reynolds number on WAF rolling moment coefficient, $\alpha = 0$, $t/C = 3$ percent.

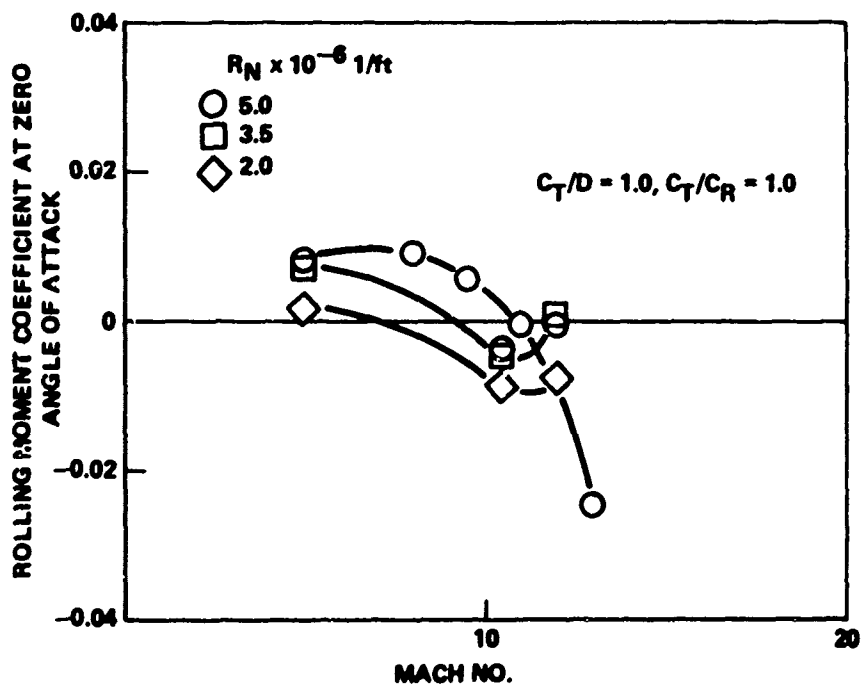


Figure 16. Effect of Reynolds number on WAF rolling moment coefficient for stepdown body, $\alpha = 0$, $t/C = 3$ percent.

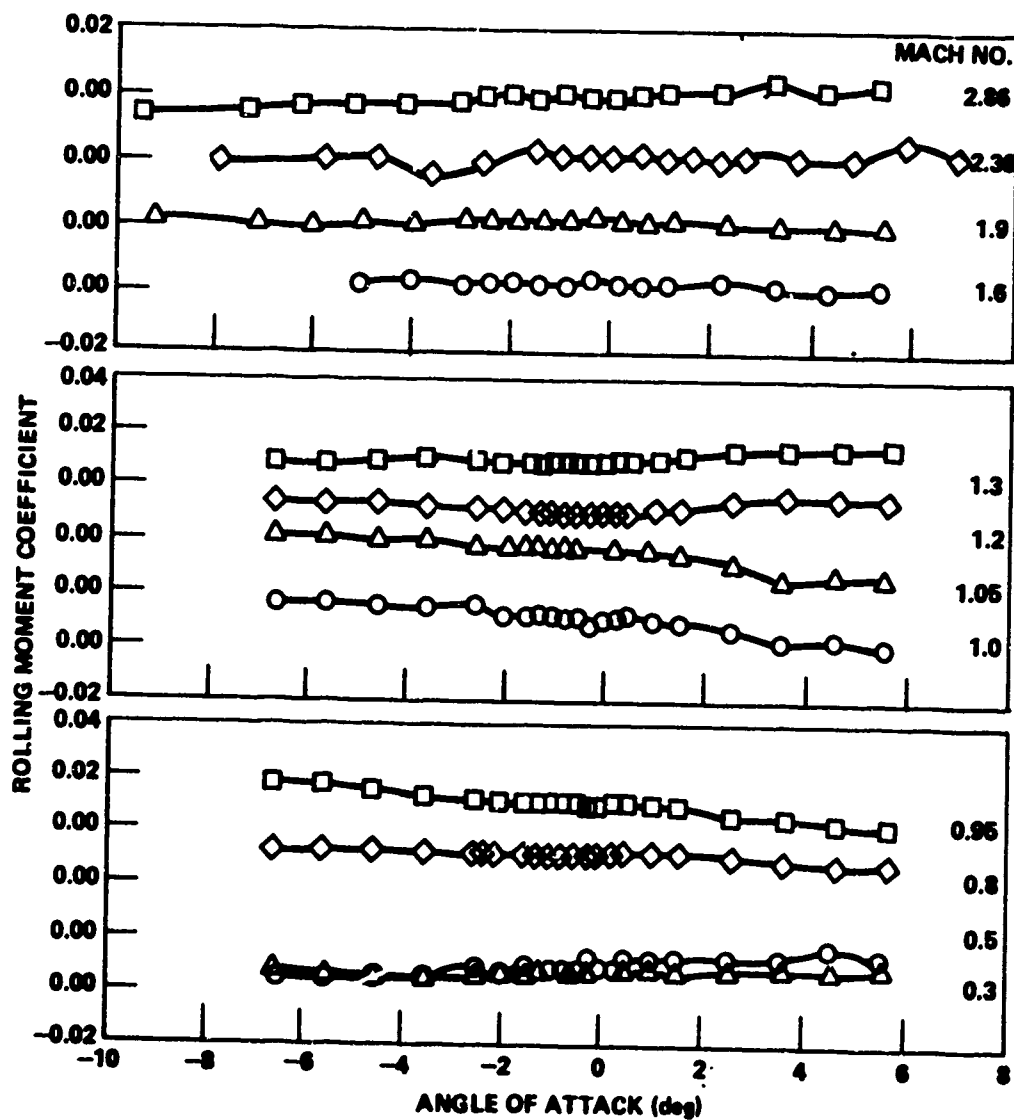


Figure 17. Variation of flat fin rolling moment with angle of attack, $AR = 0.75$, $C_T/C_R = 1.00$, $C_R/D = 1.75$.

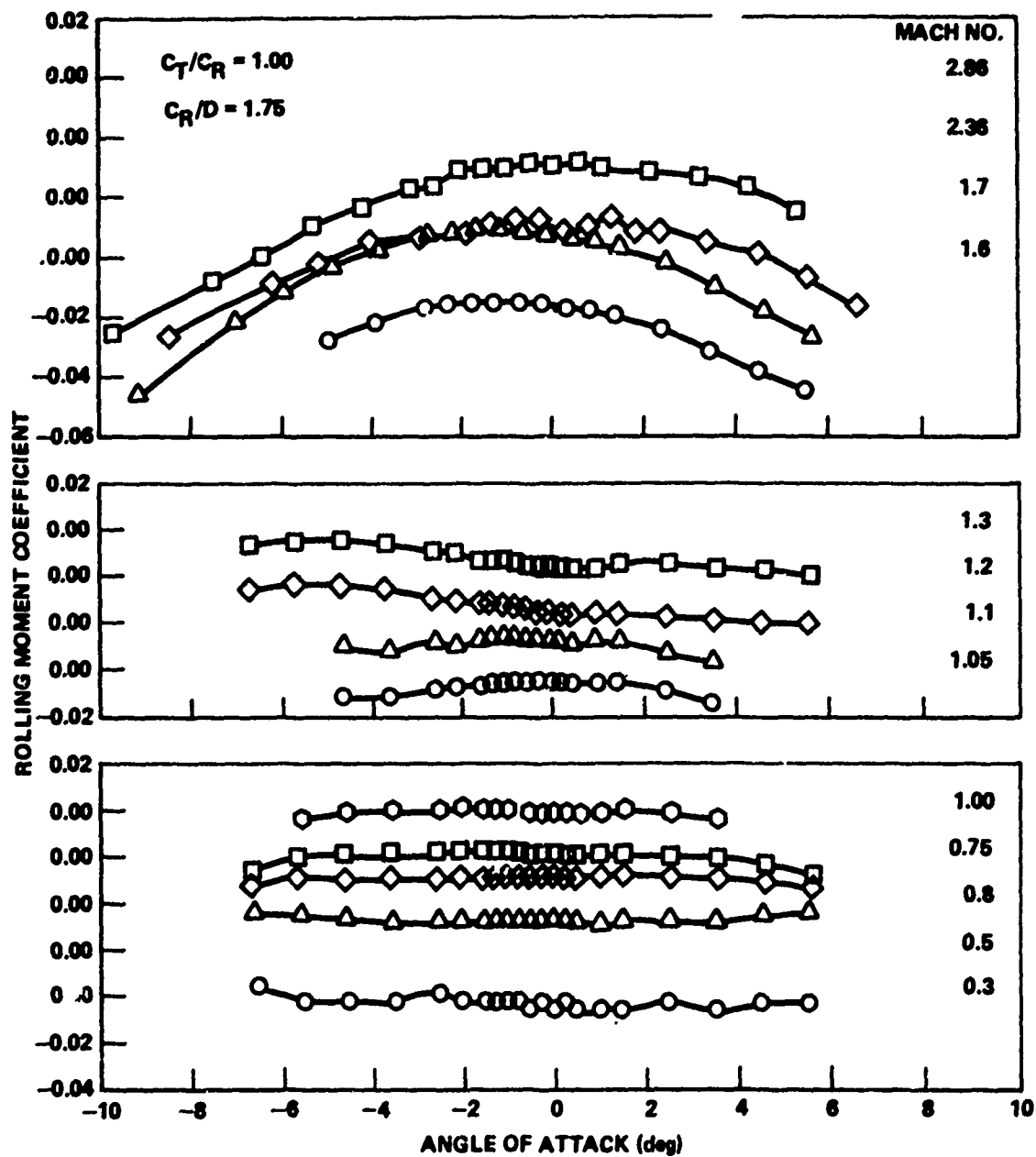


Figure 18. Variation of WAF rolling moment coefficient with angle of attack, $AR = 0.75$.

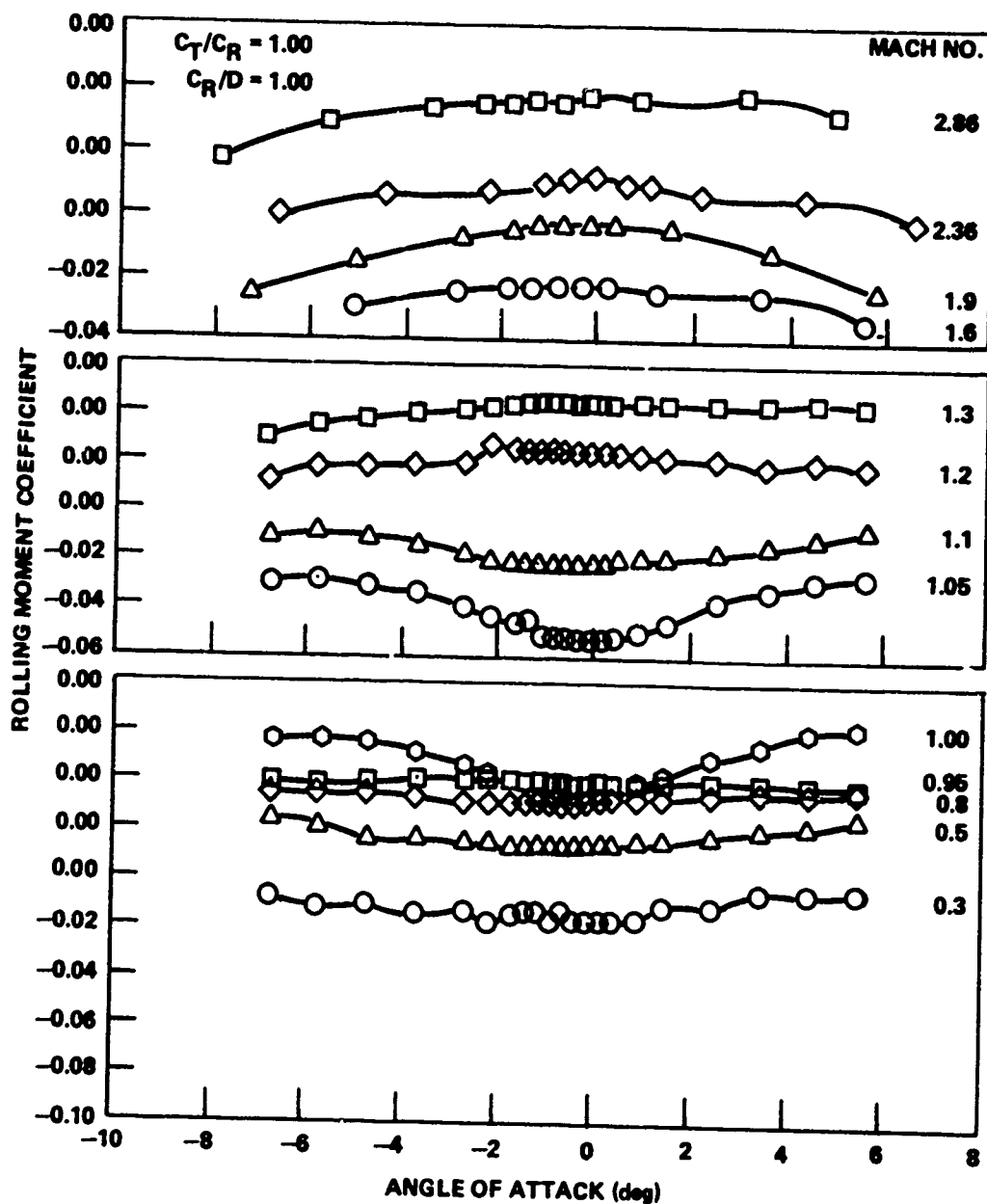


Figure 19. Variation of WAF rolling moment coefficient with angle of attack, AR = 1.33.

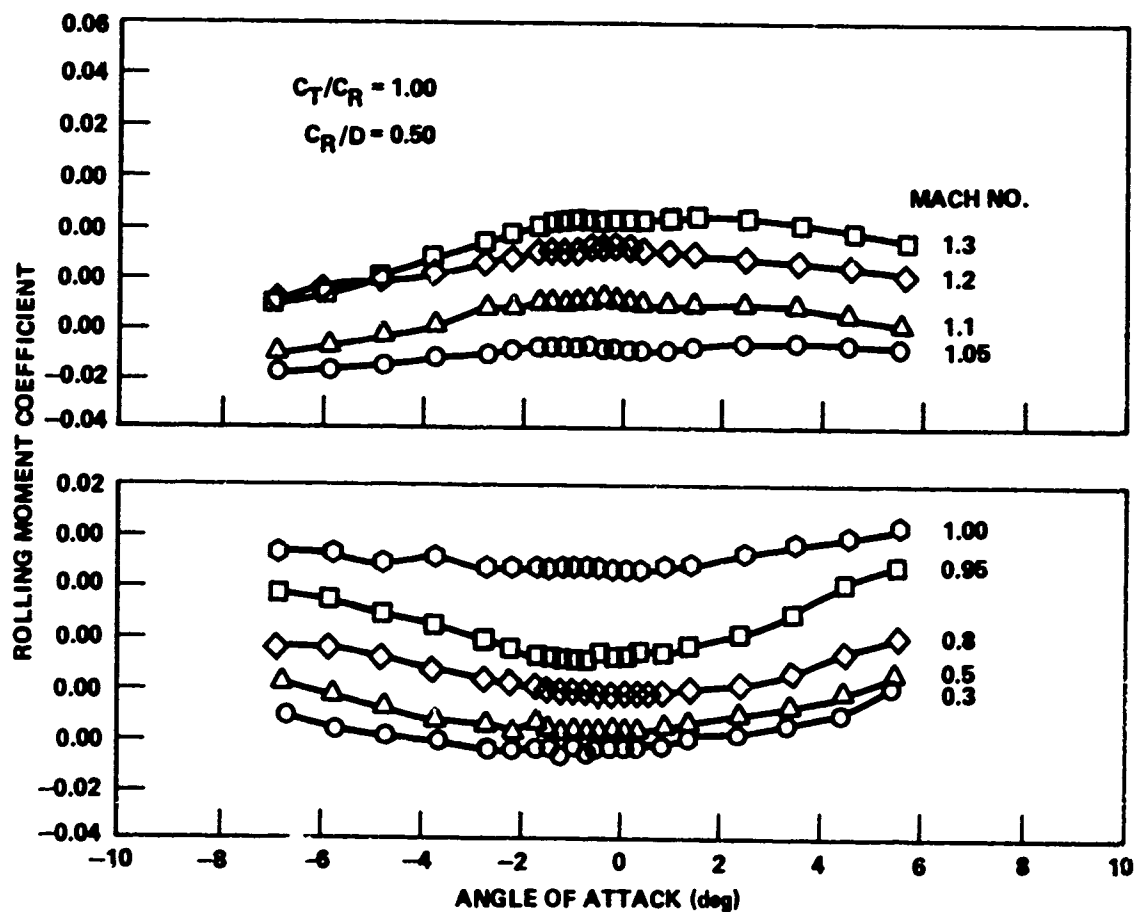


Figure 20. Variation of WAF rolling moment coefficient with angle of attack, $AR = 2.66$.

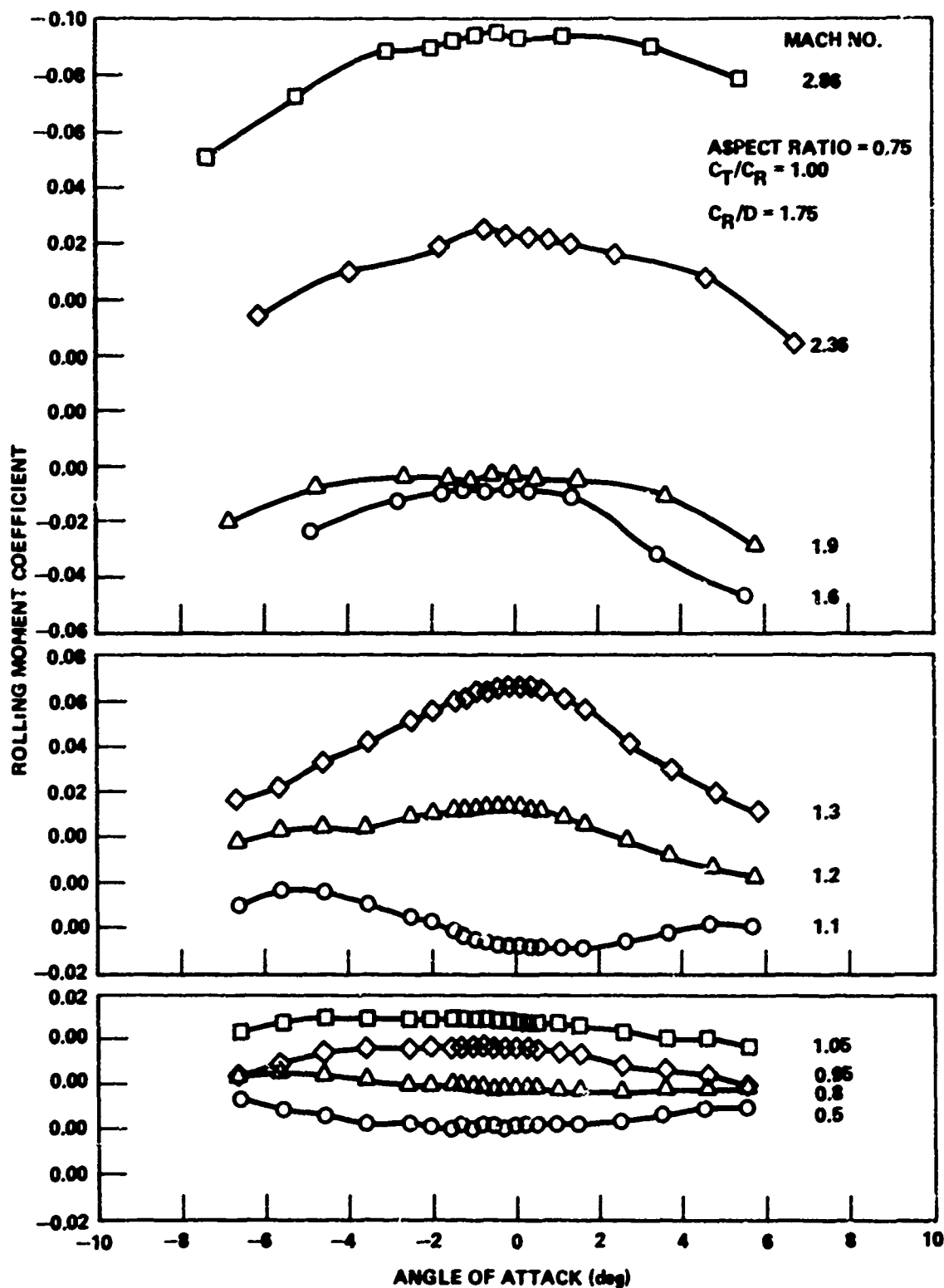


Figure 21. Variation of WAF rolling moment coefficient with angle of attack, unsymmetrical leading edge.

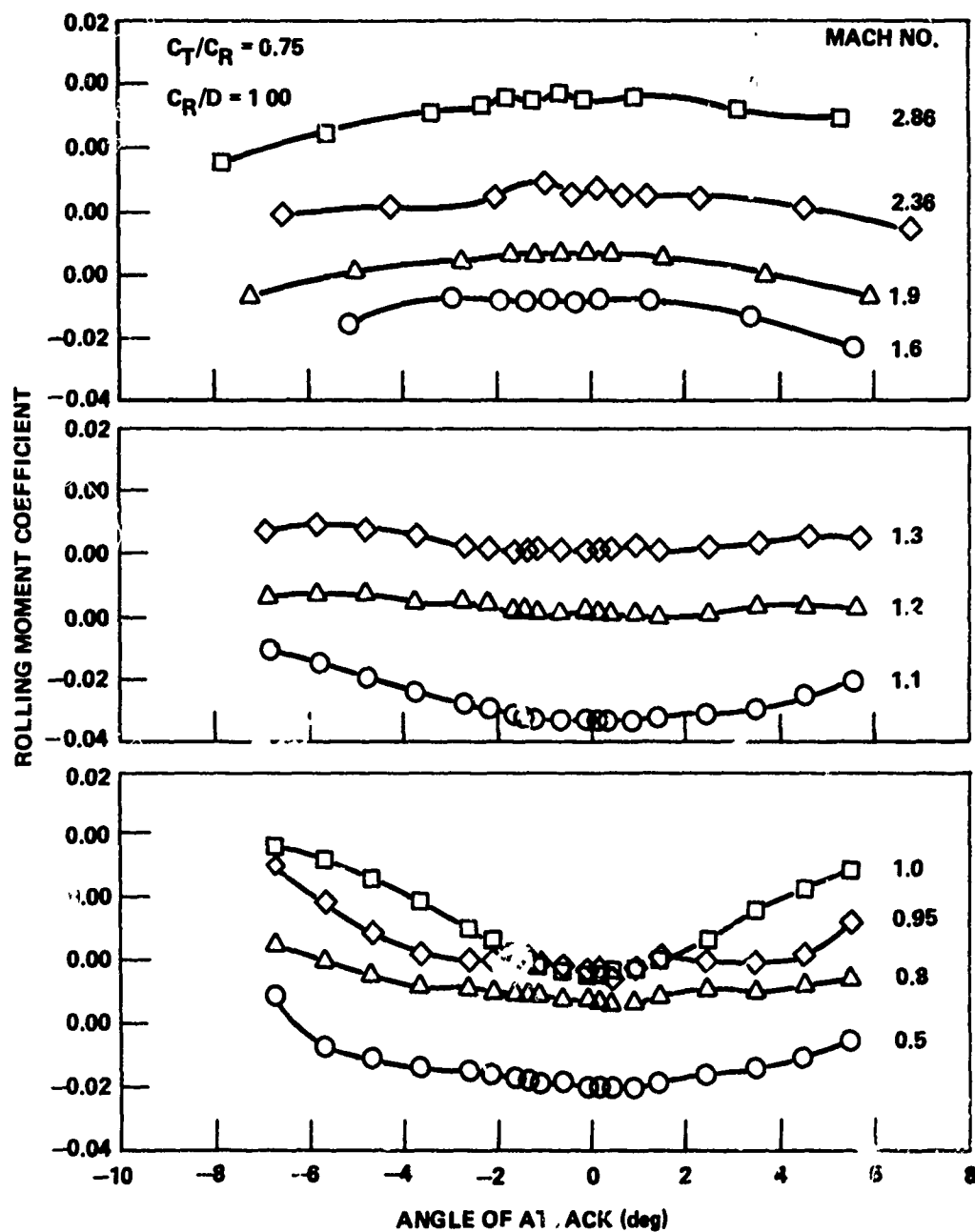


Figure 22. Variation of WAF rolling moment coefficient with angle of attack, swept leading edge.

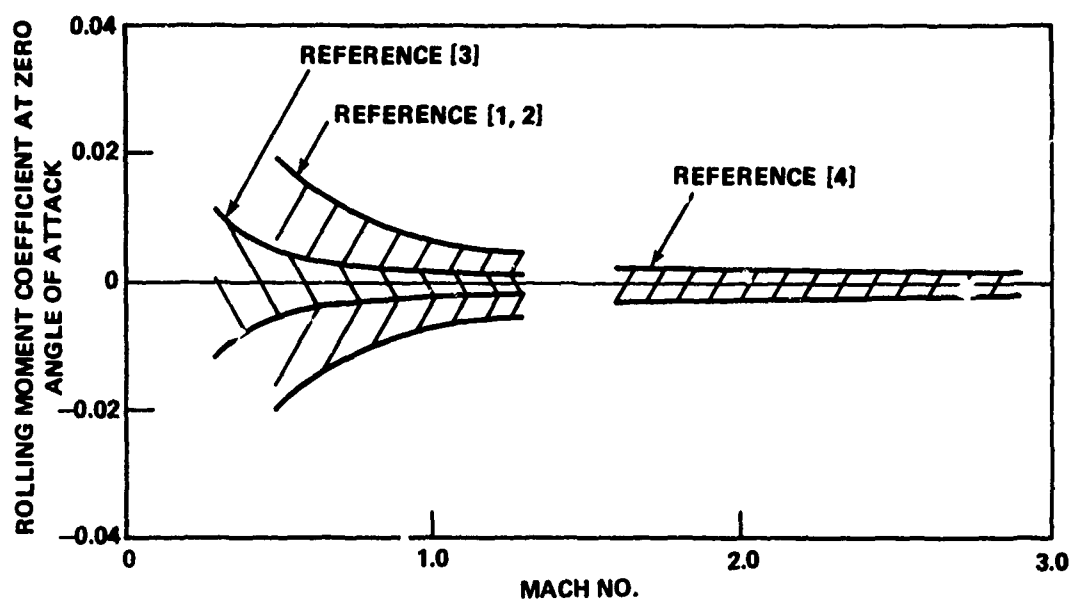


Figure 23. WAF rolling moment data precision.

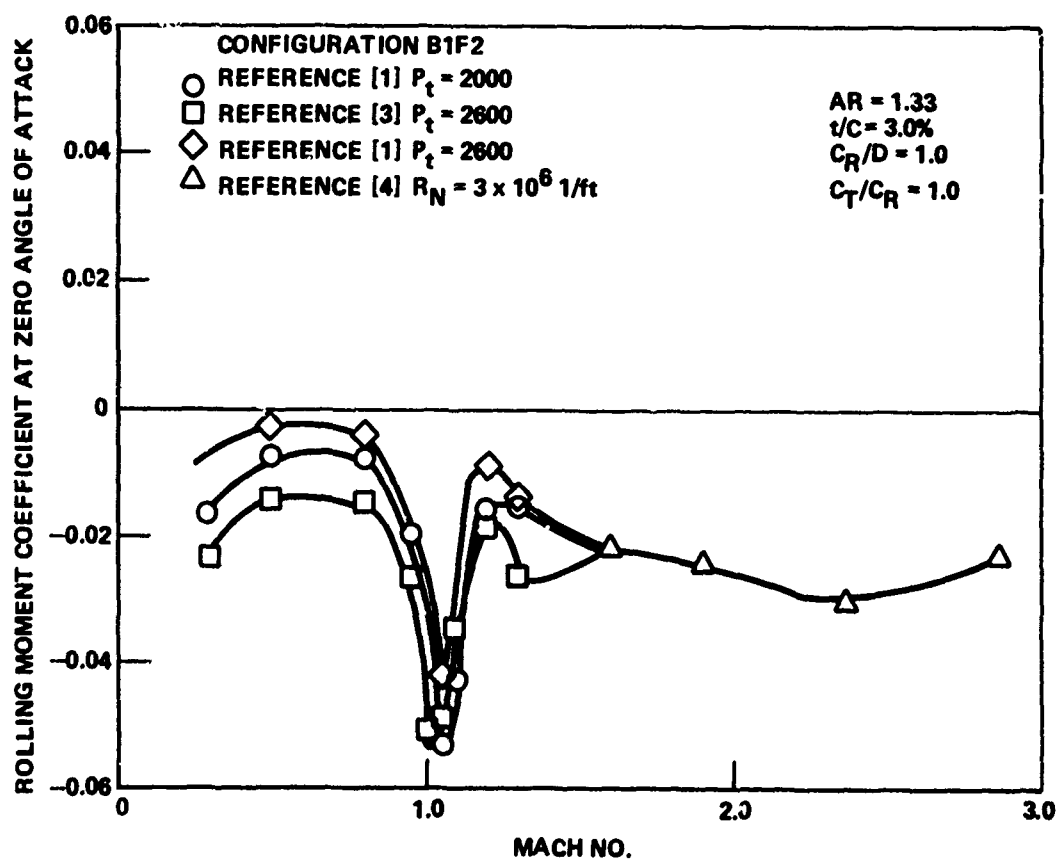


Figure 24. WAF rolling moment coefficient comparisons from several test, $\alpha = 0$, $\phi = 0$.

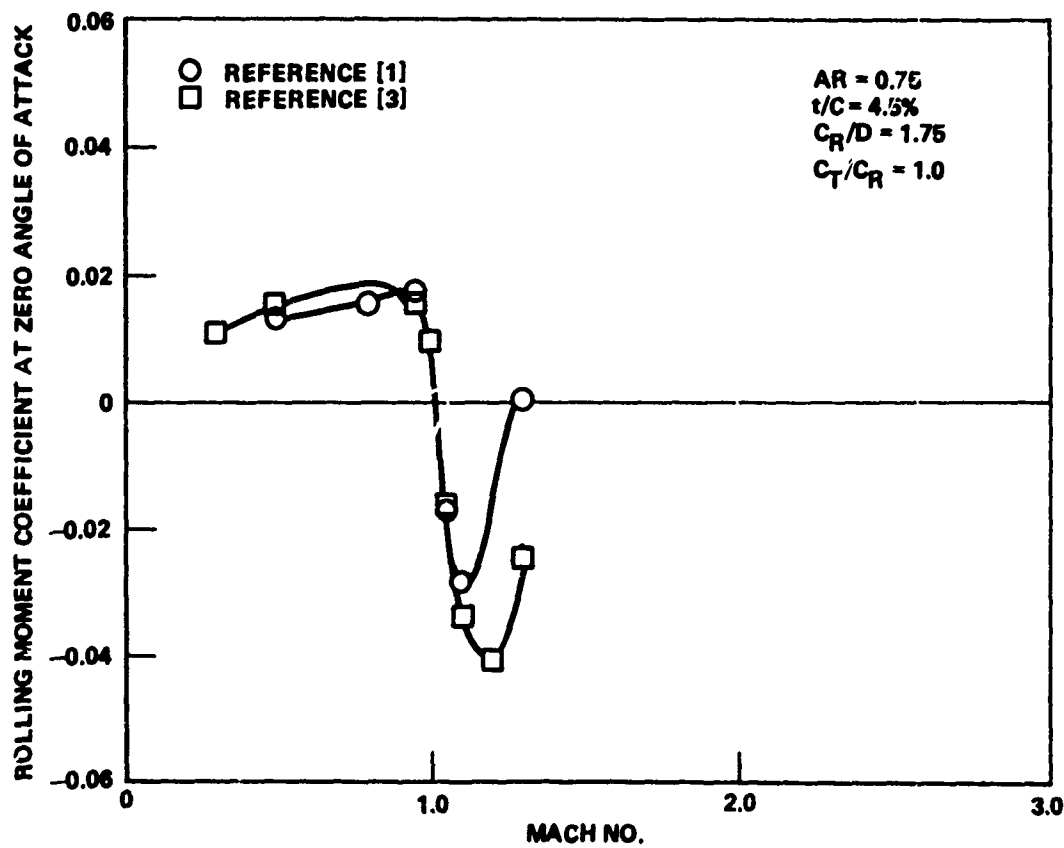
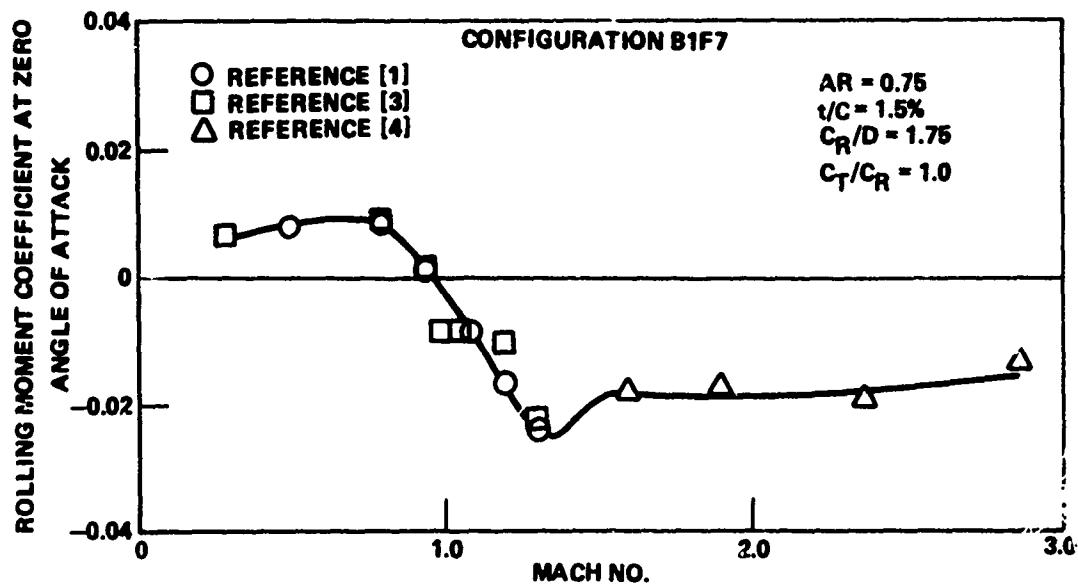


Figure 24. Concluded.

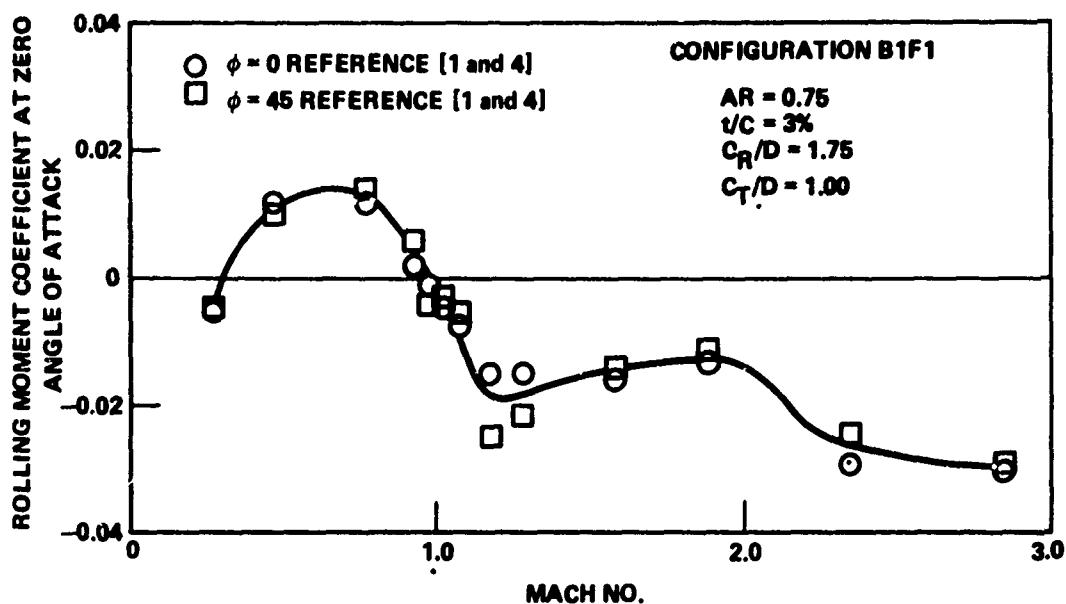


Figure 25. Roll attitude effects on WAF roll moment coefficient, $\alpha = 0$.

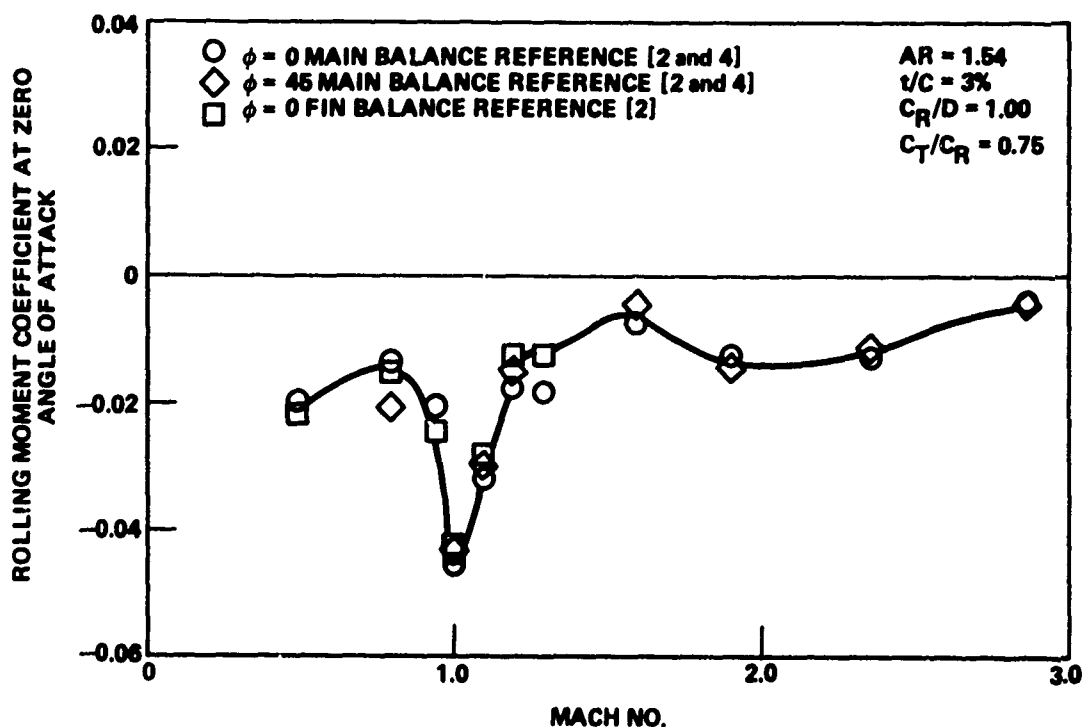


Figure 26. WAF roll moment coefficient from main balance and fin balances, $\phi = 0$ and 45 degrees.

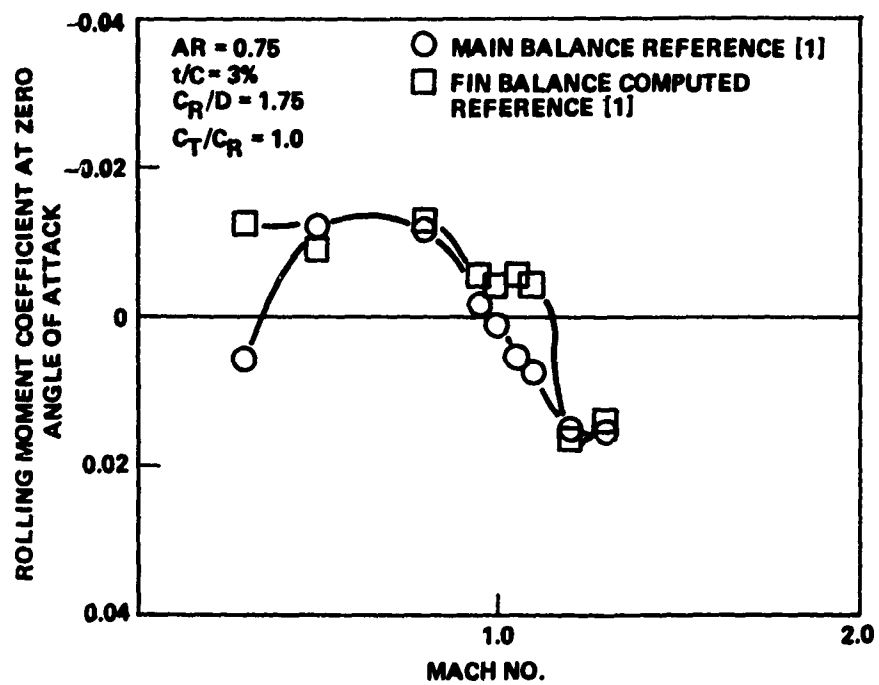


Figure 27. WAF roll moment coefficient from main balance and fin balances, $\phi = 0$.

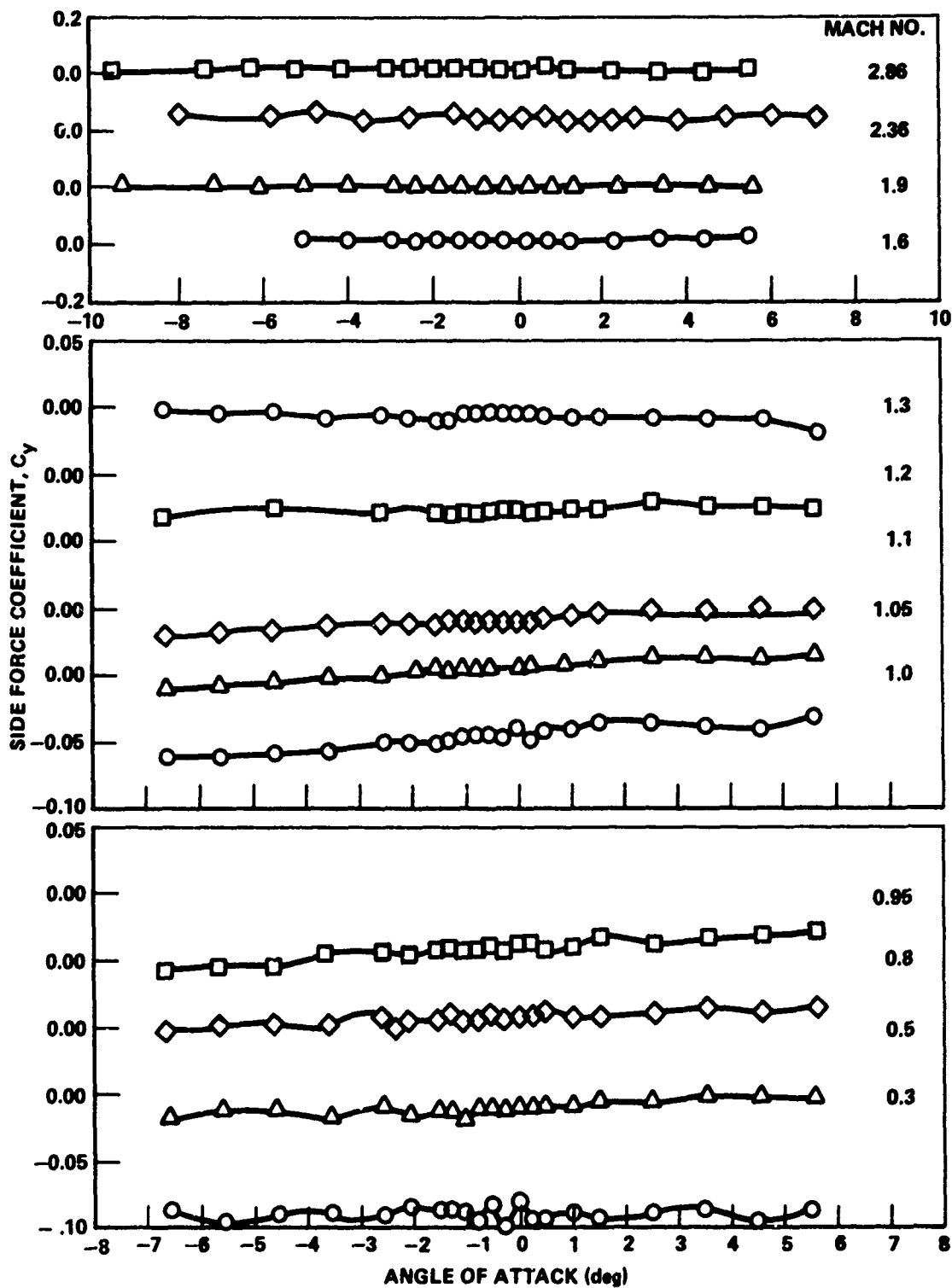


Figure 28. Variation of side force coefficient with angle of attack, flat fin, $AR = 0.75$, $C_R/D = 1.75$, $C_T/C_R = 1.00$, $\phi = 0$.

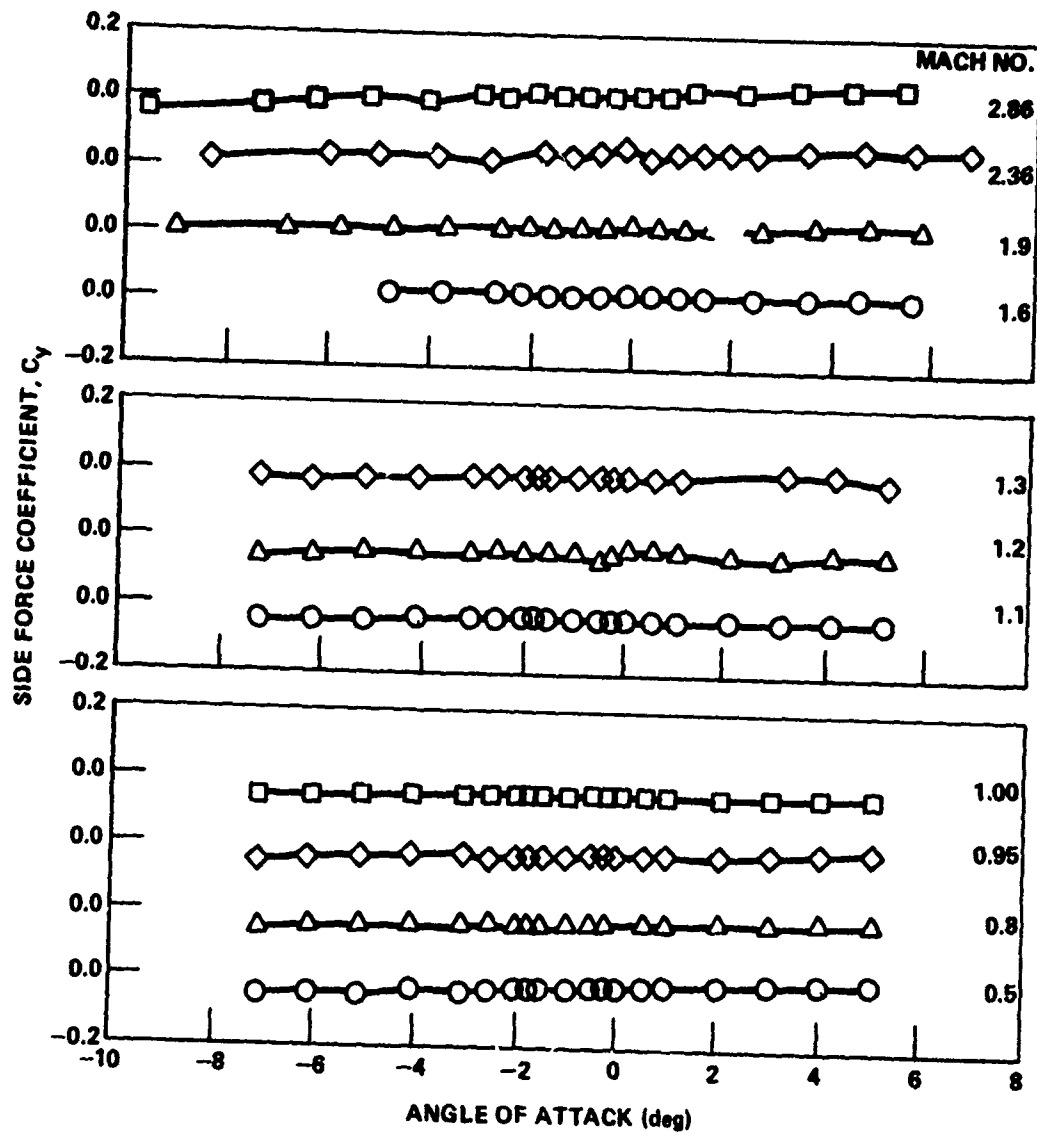


Figure 29. Variation of side force coefficient with angle of attack, WAF, $AR = 0.75$, $C_T/C_R = 1.00$, $C_R/D = 1.75$, $\phi = 0$.

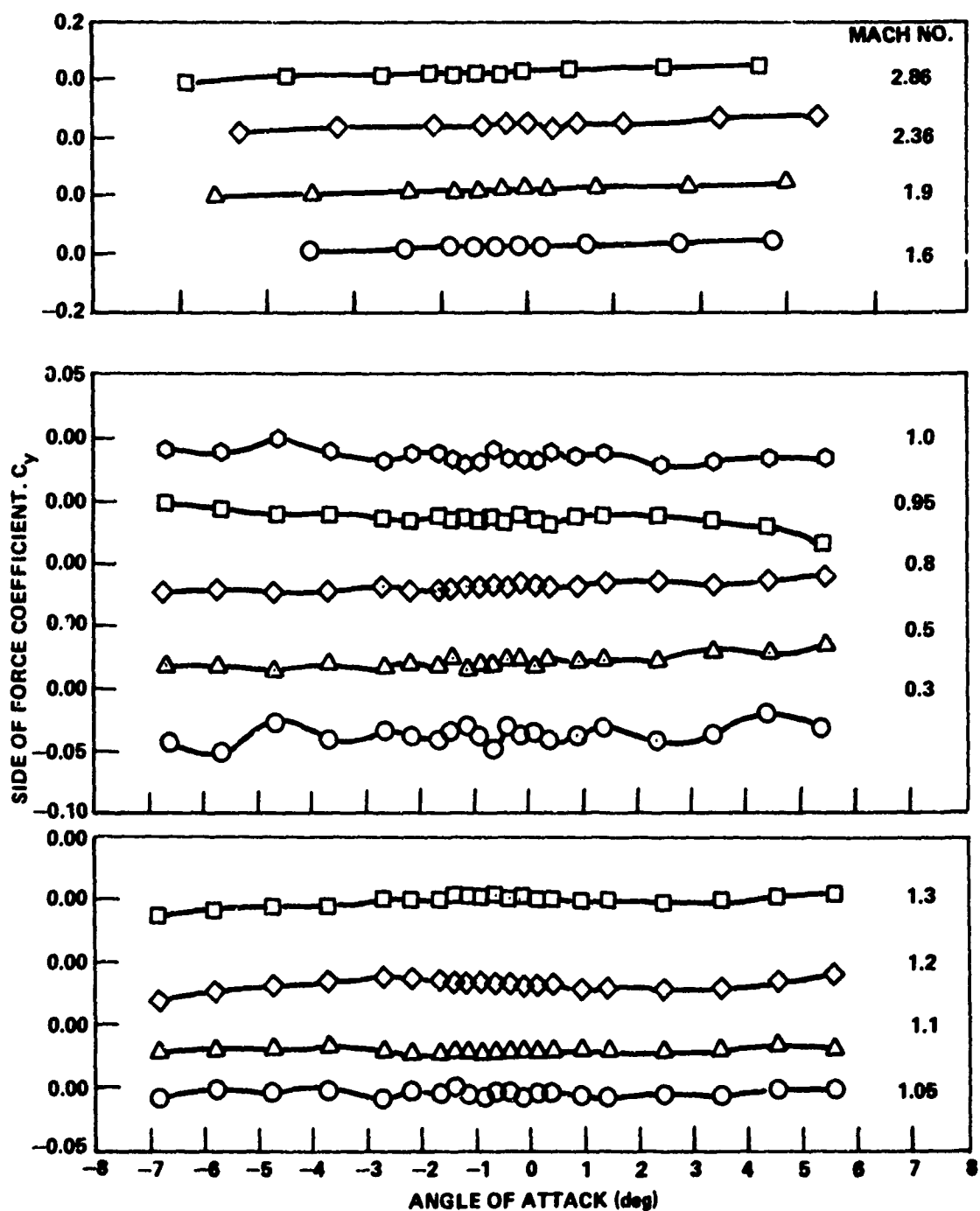


Figure 30. Variation of side force coefficient with angle of attack, WAF, $AR = 1.33$, $C_R/D = 1.00$, $C_T/C_R = 1.00$, $\phi = 0$.

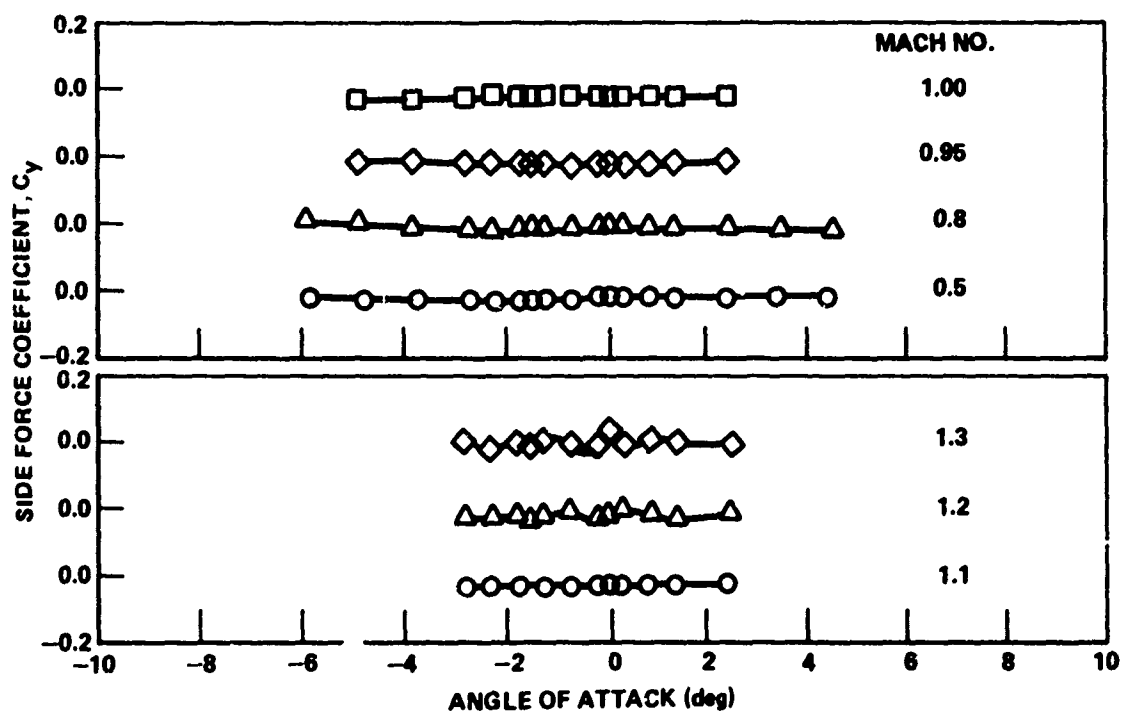


Figure 31. Variation of side force coefficient with angle of attack, WAF, $AR = 2.66$, $C_R/D = 0.50$, $C_T/C_R = 1.0$, $\phi = 0$.

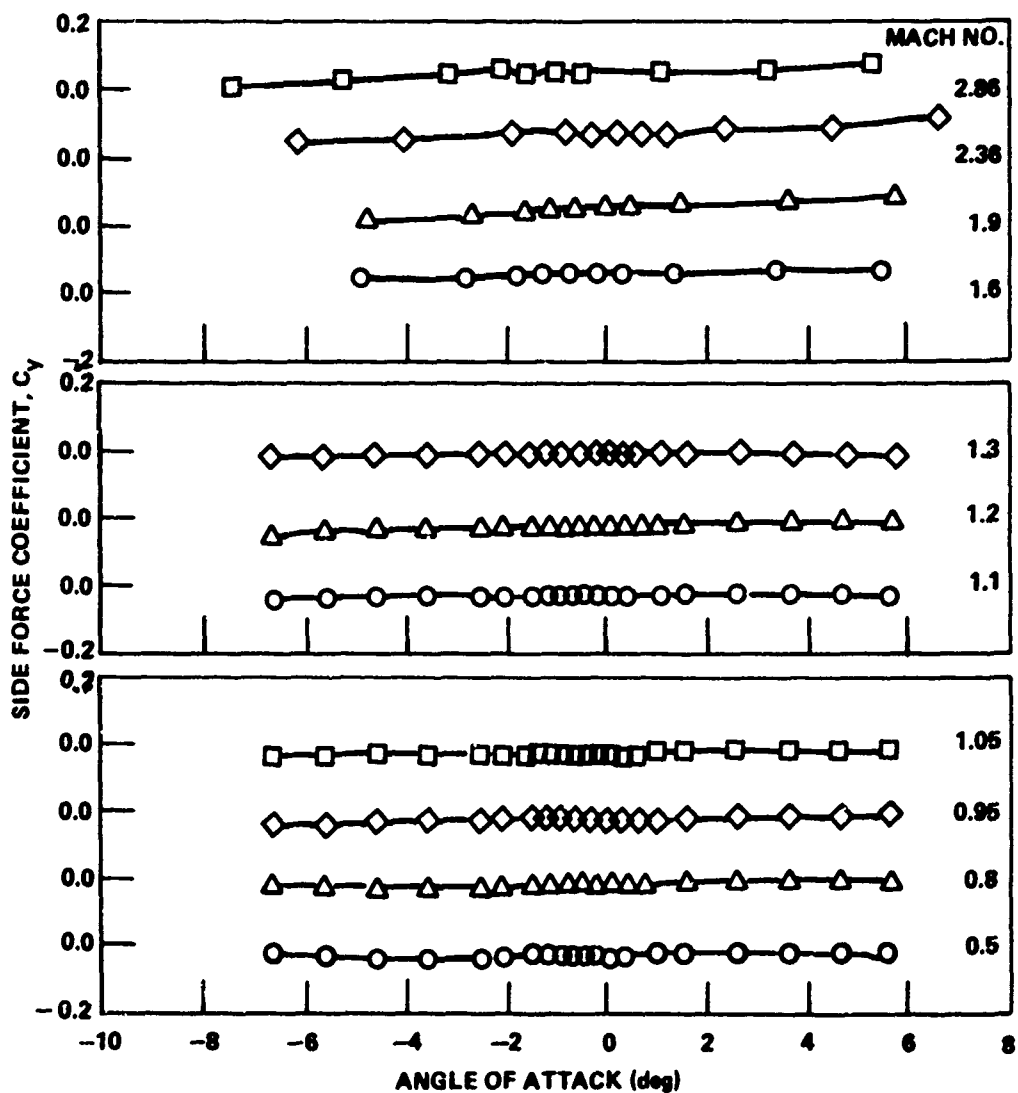


Figure 32. Variation of side force coefficient with angle of attack, WAF, $AR = 0.75$, $C_R/D = 1.0$, $C_T/C_R = 1.0$, unsymmetrical leading edge, $\phi = 0$.

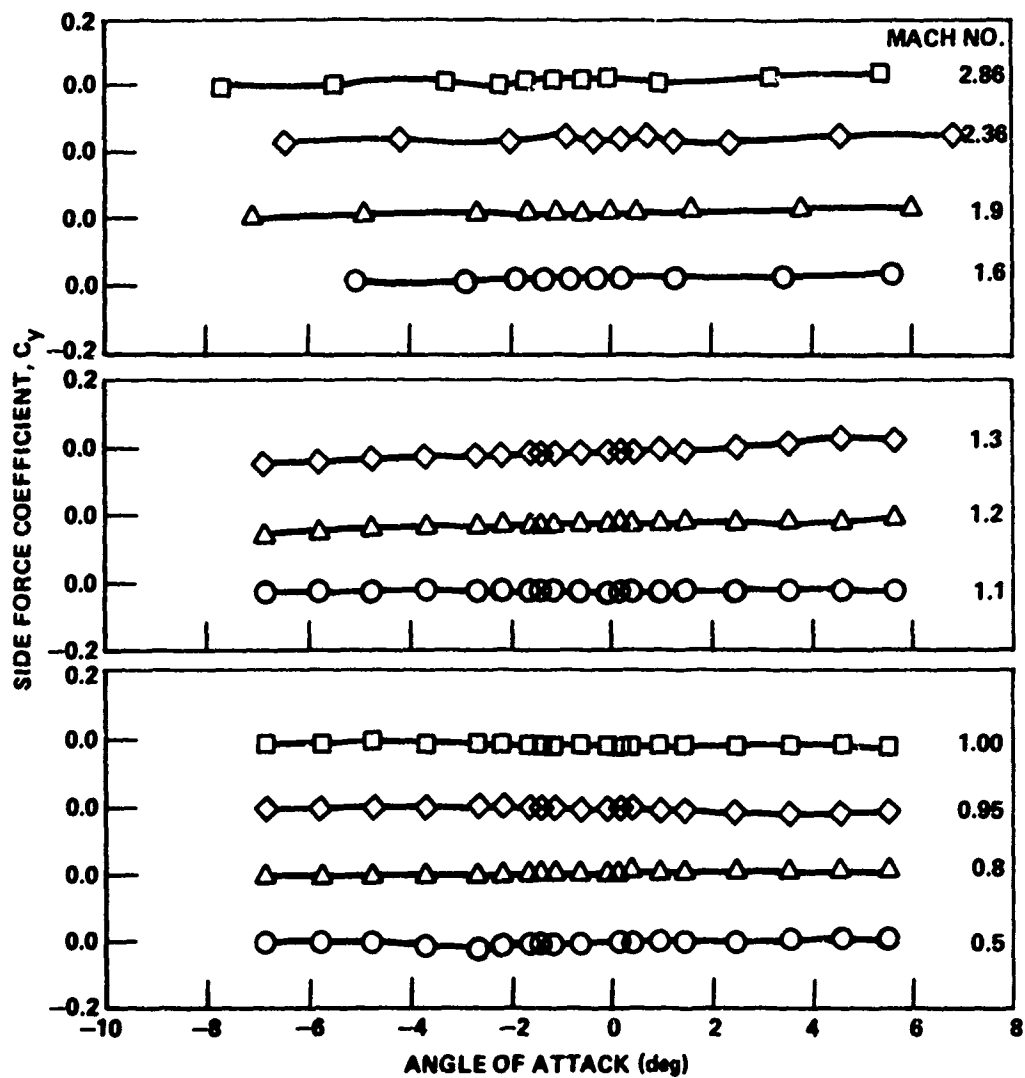


Figure 33. Variation of side force coefficient with angle of attack, WAF, $C_R/D = 1.0$, $C_T/C_R = 0.75$, $\phi = 0$.

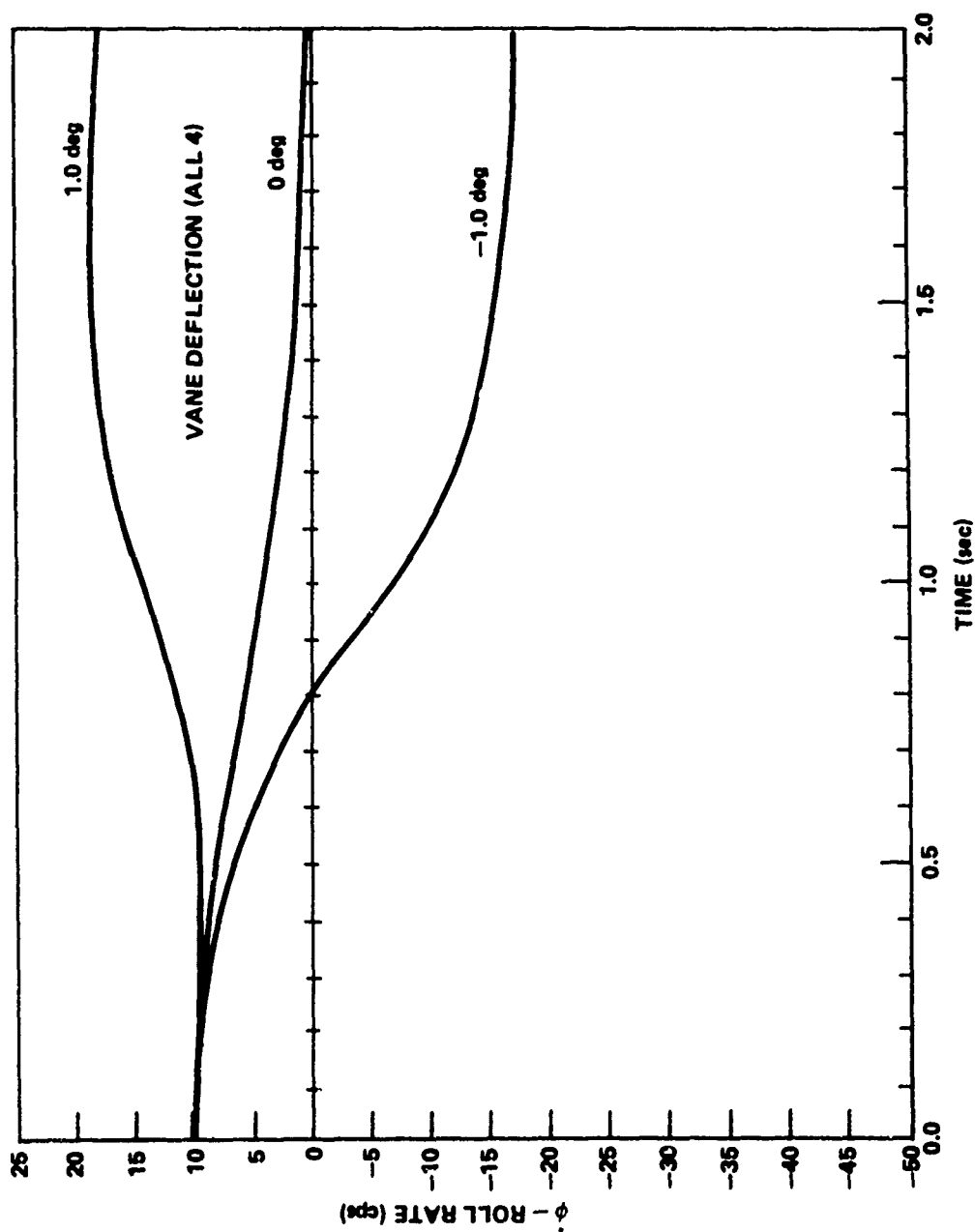


Figure 34. Effect of cant on missile roll rate, flat fin, $\dot{\phi} = 10.0$.

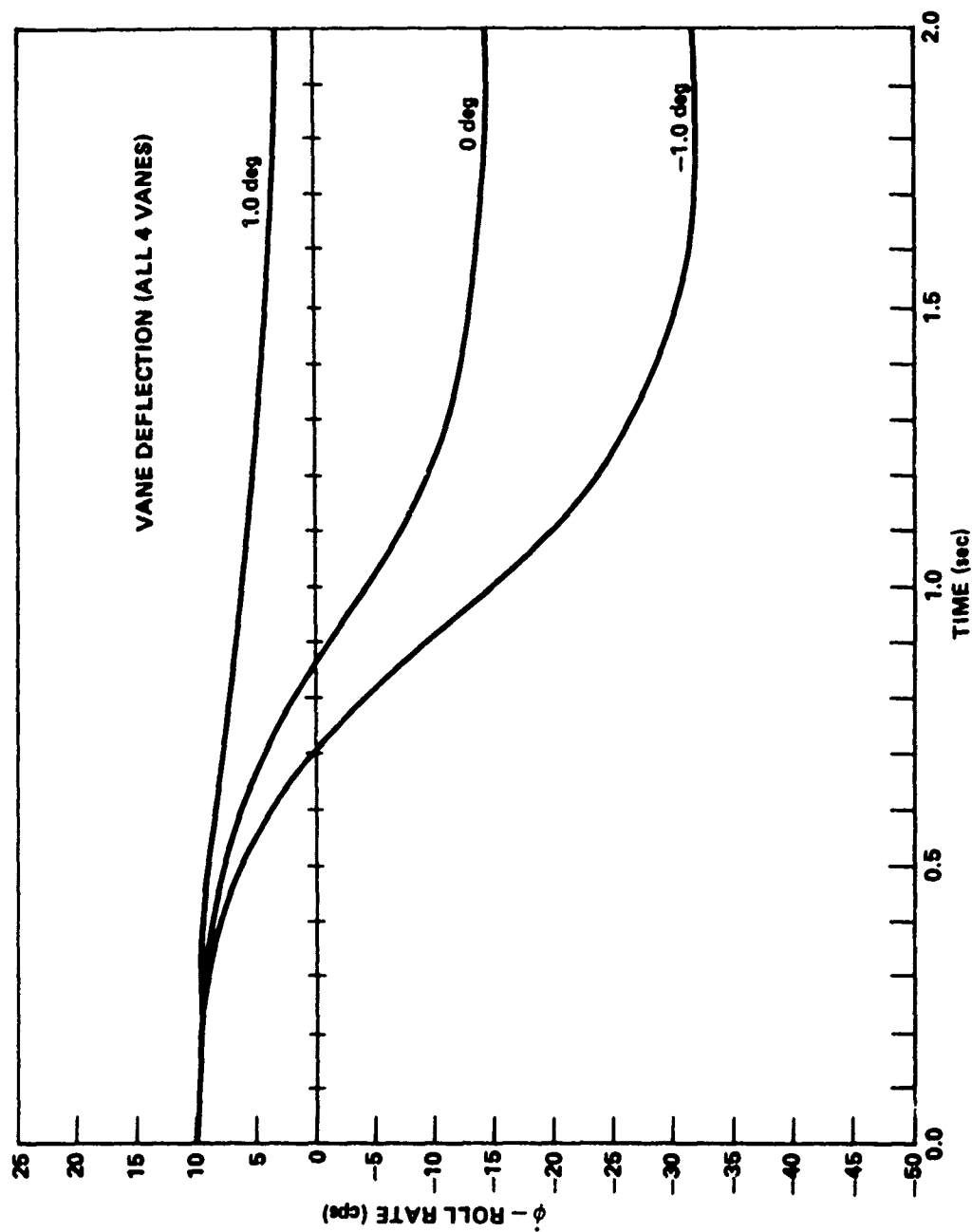


Figure 35. Effect of cant on missile roll rate, WAF, $\dot{\phi} = 10.0$.

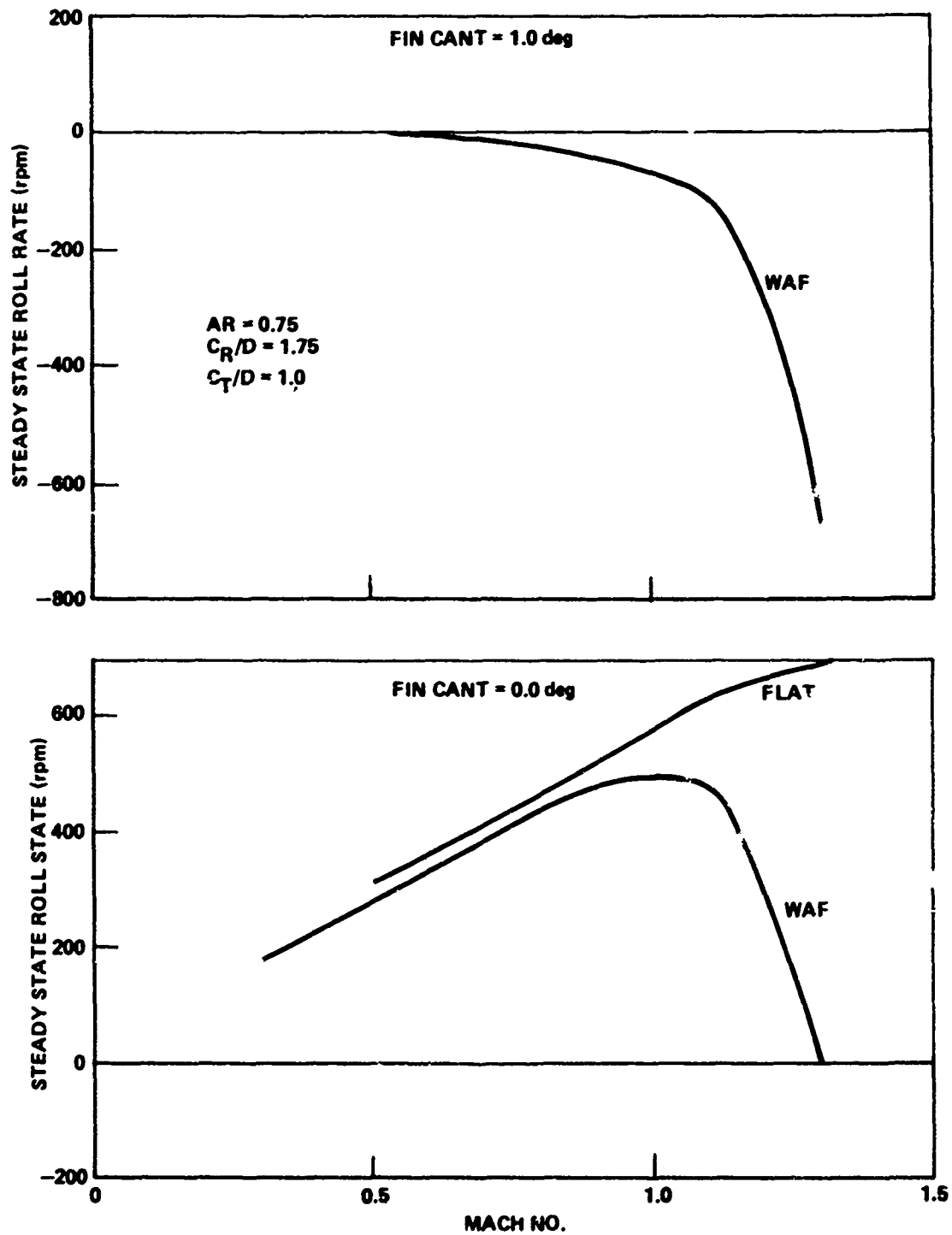


Figure 36. Experimental steady state roll rate of WAF and flat fin with fin cant.

REFERENCES

1. Dahlke, C. Wayne and Craft, J. C., Aerodynamic Characteristics of Wraparound Fins Mounted on Bodies of Revolution and Their Influence on the Missile Static Stability at Mach Numbers from 0.3 to 1.3, Vol I and Vol II, US Army Missile Command, Redstone Arsenal, Alabama, March 1972, Report No. RD-TM-72-1.
2. Dahlke, C. Wayne and Craft, J. C., Static Aerodynamic Stability Characteristics of a Body of Revolution with Wraparound Fins at Mach Numbers from 0.5 to 1.3, US Army Missile Command, Redstone Arsenal, Alabama, June 1972, Report No. RD-TM-72-6.
3. Dunkin, O. L., Influence of Curved-Fin Stabilizers on the Rolling-Moment Characteristics of 10-Cal Missiles at Mach Numbers from 0.2 to 1.3, Propulsion Wind Tunnel Facility, Arnold Engineering Development Center, Air Force Systems Command, Arnold Air Force Station, Tennessee, October 1971, AEDC-TR-71-237.
4. Dahlke, C. Wayne and Craft, J. C., Static Aerodynamic Stability Characteristics of Bodies of Revolution with Wraparound Fins at Mach Numbers from 1.6 to 2.86, US Army Missile Command, Redstone Arsenal, Alabama, September 1972, Report No. RD-TM-72-14.
5. Featherstone, H. A., The Aerodynamic Characteristics of Curved Tail Fin, Convair/Pomona, Convair Division of General Dynamics Corporation, 26 September 1960, ERR-PO-019.
6. Dahlke, Calvin W., Aerodynamics of Wrap-Around Fins, A Survey of the Literature, US Army Missile Command, Redstone Arsenal, Alabama, March 1971, Report No. RD-TR-71-7.
7. Whorric, J. M., Aerodynamic Characteristics of Several Low Aspect Ratio Stabilizer Fins at Mach Numbers from 0.8 to 1.3, Propulsion Wind Tunnel Facility, Arnold Engineering Development Center, Air Force Systems Command, Arnold Air Force Station, Tennessee, September 1972, AEDC-TR-72-143, AFATL-TR-72-189.